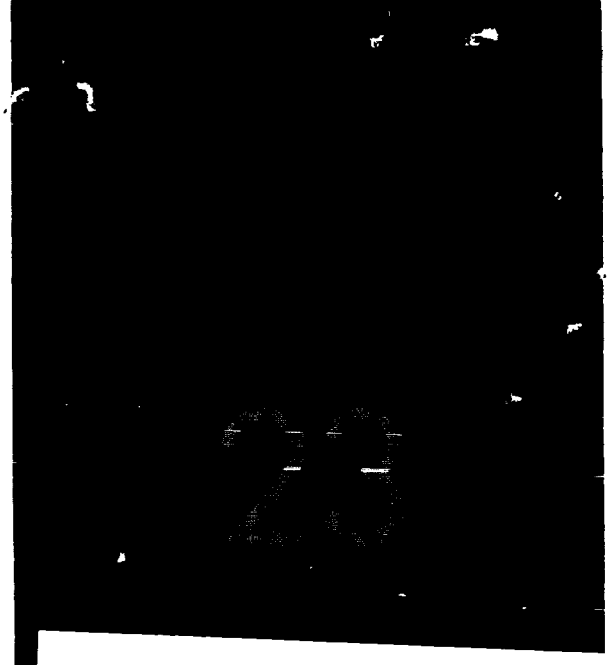

Components Irradiation Test 13

THERMISTORS

Georgia Nuclear Laboratories

LOCKHEED-GEORGIA COMPANY -- A Division of Lockheed Aircraft Corporation

ER 7899

COMPONENTS IRRADIATION TEST NO. 13
2N2501 TRANSISTORS
TI 551 DIODES AND VARIOUS TYPES OF THERMISTORS

April 1965

Prepared For:

GEORGE C. MARSHALL SPACE FLIGHT CENTER

Prepared By:

GEORGIA NUCLEAR LABORATORIES

GEORGIA NUCLEAR LABORATORIES
Lockheed-Georgia Company - A Division of Lockheed Aircraft Corporation

FOREWORD

This report is submitted to the Astrionics Laboratory of the George C. Marshall Space Flight Center, National Aeronautics and Space Administration, Huntsville, Alabama, in accordance with the requirements of Task Order No. ASTR-LGC-23 of Contract No. NAS 8-5332. The report is one of a series describing radiation effects on various electronic components. This particular report concerns one type of transistor, one type of diode and nine types of thermistors. The tests were performed by the Georgia Nuclear Laboratories, Dawsonville, Georgia.

TABLE OF CONTENTS

LIST OF TABLES AND FIGURES

LIST OF TABLES AND FIGURES
(Continued)

LIST OF TABLES AND FIGURES
(Continued)

1.0 SUMMARY

Twenty (20) specimens of the type 2N2501, General Instrument, transistor and 20 specimens of the type TI 551, Texas Instruments, diode were subjected to a nuclear radiation environment at 30° C. Also subjected to the same radiation environment at 0° C were the following thermistors:

No.	Type	Manufacturer
5	A0610P-13	Carborundum
5	A1406P-13	Carborundum
5	R172	General Electric
5	GB31L1	Fenwal
5	GB41L1	Fenwal
5	RL13M1	Keystone
5	RL20E1	Keystone
5	RL4M1	Keystone
5	RL7E1	Keystone

Measurements were made to determine the effect of the radiation on the h_{FE}, h_{ie} and I_{CBO} parameters of the transistors, the V_F and I_R parameters of the transistors, the V_F and I_R parameters of the diodes, and the resistance (temperature indication) of the thermistors.

The test data indicated:

For the 2N2501 transistor

(1) All specimens failed (50% decrease in h_{FE}). The range of failures extended from 6.4×10^{12} n/cm^2 to 2.6×10^{13} n/cm^2.

(2) Normalized h_{ie} decreased at a slightly greater rate than did normalized h_{FE}.

(3) I_{CBO} was increased by the irradiation, but not beyond 0.11 μA for any specimen.

For the TI 551 diode

(1) Both V_F and I_R were increased by the irradiation.

(2) No specimen showed an increase in V_F as great as 100%.

(3) All specimens failed ($I_R > 0.2\ \mu A$) because of increase in I_R. Failures ranged from 9.0×10^{13} n/cm^2 to 6.3×10^{14} n/cm^2.

For the thermistors

(1) Only one group contained specimens which all showed permanent radiation effect. This was the A0610P-13 group.

(2) Three groups contained one or two specimens each which showed permanent radiation effect. These were the R172, GB41L1, and the RL20E1 groups.

2.0 INTRODUCTION

The experiment described in this report is the thirteenth irradiation of electronic components and is the seventeenth in a series of radiation effects tests on electronic equipment, circuits, and components contemplated for use on a nuclear space vehicle. Since the use of equipment on this vehicle is contingent upon its ability to withstand the nuclear environment, the Astrionics Laboratory of the Marshall Space Flight Center has undertaken to assure that Government furnished or specified equipment will survive this environment. The equipment is to be subjected to the expected nuclear environment as simulated at the Georgia Nuclear Laboratories. Measurements made on the equipment during the irradiation will describe its radiation tolerance.

The subjects of this test are the type 2N2501 transistor, the type TI 551 diode and various types of thermistors.

3.0 TEST PROCEDURE

The test specimens were supplied by the Astrionics Laboratory of the Marshall Space Flight Center. During the test the semiconductor specimens were mounted in a controlled temperature chamber adjusted to hold the temperature at 30 $\pm$ 2° C. The thermistor specimens were immersed in an ice bath contained in two Dewar flasks inserted in a block of styrofoam. The specimens were first exposed to a nominal gamma dose of 5.7×10^5 r behind a neutron attenuator shield. The shielding was then removed and the test was continued until a nominal integrated neutron flux of 6.9×10^{14} n/cm^2 was accumulated. At this point the reactor was shut down for a period of about 17 hours. At the end of the shutdown period the test was resumed, and continued until a total nominal gamma dose of 1.44×10^7 r and a total nominal integrated neutron flux of 1.85×10^{15} n/cm^2 were accumulated. Before, during and after the irradiation, measurements were made to determine the parameters listed in Table 1. Measurements were also made during the test to define the nuclear and temperature environments.

3.1 TEST SPECIMENS

The specimens tested are listed in Table 1. The semiconductor specimens were mounted on printed circuit boards by the Astrionics Laboratory. The thermistor specimens were mounted by GNL. All specimens were new units and had only been subjected to MSFC receiving inspection. Manufacturers' specifications for the specimens are shown in Table 2. The specimen boards were mounted vertically in the radiation field to equalize the radiation flux distribution. Figures 1, 2 and 3 show the relative positions of the specimens. The environmental chamber in which the specimens were placed was located directly adjacent to the reactor for the irradiation.

3.2 TEST SPECIMEN MEASUREMENTS

A complete set of data was taken prior to reactor startup to establish baseline data for the test. During the irradiation, measurements were made at all reactor power settings. Measurements were also made:

a. during reactor shutdown for removal of the shield,
b. at the beginning and the end of the 17-hour reactor shutdown period,
c. upon completion of the irradiation, and
d. approximately 66 hours after the end of the irradiation (transistors excepted).

All measurements were performed with the test fixture in place at the reactor facility.

3.3 INSTRUMENTATION

3.3.1 Transistor Measurement Circuits

The transistor measurement circuits are shown in Figures 4 and 5. The emitters of the test specimens were commoned, and the base and collector were commutated into the test circuits.

In the h_{FE} and h_{ie} measurement circuits (Figure 5) the feedback loop, including amplifier A, establishes the base current necessary to provide the collector current shown in Table 1. Capacitors of 910 picofarads were connected from collector to emitter of each specimen on the printed circuit board to prevent oscillation caused by the inductance and capacitance of the long instrumentation cables. These were mica capacitors which had previously shown tolerance in excess of the radiation levels experienced in this test. The base current was measured by the digital voltmeter and h_{FE} was calculated from these measurements. With a signal of 10 microamps at 1 kc applied to the base, the base to emitter voltage (V_{be}) was

measured by an ac voltmeter. These values were used in the determination of input impedance (h_{ie}). The maximum sensitivity for I_{CBO} measurements was in the order of 10^{-8} amps, while the system accuracy of the measurement circuit (Figure 4) was $\pm$ 1% $\pm$ 10 nanoamps.

3.2.2 Diode Measurement Circuits

The circuits shown in Figure 6 were used to perform the diode measurements with the GNL digital voltmeter data logging system. The cathodes of all diodes were commoned, and the anodes were commutated into the test circuit. Potential leads for the diode specimens were used to eliminate the voltage drop in the 300 foot instrumentation cables to the test specimens. The maximum sensitivity for reverse current measurements was in the order of 10^{-8} amps.

3.3.3 Thermistor Measurements

The circuits used in the measurement of thermistor resistance are shown in Figure 7. Using the digital voltmeter of the GNL data logging system, the output voltage of the bridge network was measured. Using this voltage, the value of the precision resistor, R_p and the bridge voltage, E, the resistance R_x of the thermistor was calculated. The current limiting resistors were chosen so that the power dissipation of the thermistors was less than 0.1 times the dissipation constant ($\leq 0.1^{\circ}$ C). The system accuracy of the measurement circuits was $\pm$ 0.5%, while sensitivity for each thermistor measurement was as follows:

Type	System Sensitivity (ohm)	Thermistor Sensitivity ohm/0.1° C	Nominal Resistance at 0° C (ohm)
R 172	± 1.3	52.5	15 k
A0610P	± 0.4	1.6	500
A 1406P	± 0.10	0.20	62.5
GB 31L1	± 1.8	10.5	2.9 k
GB 41L1	± 8.0	105	29 k
RL 7E1	± 0.7	8.5	3.2 k
RL 20E1	± 3.0	96	33 k
RL 4M1	± 0.04	0.16	61
RL 13 M1	± 0.11	0.89	310

3.4 TEST ENVIRONMENT

3.4.1 Pressure

During the test all specimens were at atmospheric pressure.

3.4.2 Temperature

The transistor and diode specimens were located in an environmental chamber at a temperature of 30 ± 2° C during the test. Near the end of the test the temperature increased because of gamma heating. See Figures 8 and 9 for the temperature traces for these specimens. The thermistor specimens were immersed in ice baths contained in two separate Dewar flasks. During the latter part of the test the ice in the baths melted because of gamma heating and the 17-hour shutdown period. The temperature traces for the two baths are shown in Figures 10 and 11.

3.4.3 Nuclear

The irradiation was performed in two radiation phases with a lapse of about one hour between phases. The first phase was conducted using neutron attenuation shielding interposed between the reactor and the specimens. The second phase was without shielding. This latter phase was interrupted by a period of about 17 hours at zero reactor power. The neutron to gamma ratio was 2.3×10^5 nvt/r with shielding and 1.3×10^8 nvt/r after shielding had been removed. During the irradiation both neutron and gamma radiations were monitored and recorded.* Isoline radiation flux plots were made for use in data reduction.

*A more detailed description of the GNL Nuclear Measurement System is contained in a previous report, viz., Components Irradiation Test No. 1, ER-6785, Georgia Nuclear Laboratories, Dawsonville, Georgia.

4.0 METHOD OF DATA ANALYSIS

The GNL Data Logging System recorded the parameter measurements in typewritten digital form and simultaneously punched the data in five-channel perforated tape. A tape-to-card converter was used to transfer the data to IBM cards which were then programmed into an IBM 7094 computer to yield the parameters portrayed in the included graphs.

Normalization of a parameter was accomplished by dividing each parameter value by its corresponding pre-irradiation value.

The mean parameter value for a data group, where shown, was computed by adding the individual specimen parameter values and dividing the sum by the number of specimens.

The median parameter value for a data group (that value which divides a distribution so that an equal number of items is on either side of it) was determined from a plot of the individual specimen parameter values on an arithmetic probability chart. The limits of the 68% envelopes were determined by picking off those values within which were contained 34% of the specimens next above the group median value and 34% of the specimens next below the group median value. The limits of the 95% envelopes were found in a similar fashion. The 7094 computer performed these functions.

In those cases where the parameter of an individual specimen behaved significantly differently from the group median, these "unusual" specimens have been portrayed separately.

Radiation environmental data shown on the figures' abscissae were obtained by integrating, with respect to time, the gamma dose rates and neutron fluxes.

Those figures which show "Percent Failed Versus Integrated Neutron Flux" were prepared in a manner similar to the procedure described by Mr. Frank W. Poblenz in an article entitled "Analysis of Transistor Failure in A Nuclear Environment," which appeared in Volume NS-10, Number 1, January 1963, of the IEEE Transactions on Nuclear Science. This type of presentation enables the circuit designer to predict with 50% confidence the radiation level at which any given percentage of the particular component will equal or exceed the failure criteria.

Copies of the reduced data from which the graphs were prepared are on file in the Astrionics Laboratory of the George C. Marshall Space Flight Center, NASA, Huntsville, Alabama, and in the Georgia Nuclear Laboratories, Lockheed-Georgia Company, Dawsonville, Georgia.

5.0 TEST DATA AND DISCUSSION OF RESULTS

The test data have been presented herein in graphical form. The radiation exposure is, in all cases, a combination of neutrons and gamma rays. The abscissa scale on each of the graphs is accumulated neutrons/cm^2 greater than 0.5 MeV. However, the coincident accumulated gamma dose (r) is also indicated at those points where changes in the reactor power rate occurred. It is important to remember that the total radiation exposure consists of both neutrons and gamma rays, and that each may contribute, in varying degrees, to the degradation of a component's parameter.

5.1 TYPE 2N2501 TRANSISTOR

The specimens tested were manufactured by General Instrument Corporation. The specimens were irradiated in an environmental chamber adjusted to hold the temperature at $30 \pm 2^{\circ}$ C. However, gamma heating near the end of the test caused the temperature to rise above the specified limits. Figure 8 shows the temperature trace for these specimens.

5.1.1 The h_{FE} Parameter

The initial value of h_{FE} for one specimen was considered spurious and this specimen was eliminated from the group. All specimens showed a decrease in h_{FE} of more than 50% during the irradiation. The median failure point, with failure defined as 50% decrease in h_{FE}, was about 1.8×10^{13} n/cm^2. Figure 12 shows the behavior of the normalized h_{FE} parameter for the group. The discontinuity in the slope of the median which occurred at the point of LiH shield removal indicates that the gamma irradiation contributed significantly to the degradation of h_{FE}. Figure 13 shows the failure pattern for the group.

Initial values of h_{FE} and order of failure are tabulated below:

h_{FE_o}	Order of Failure
65.12	17
68.47	16
69.68	19
71.40	10
71.90	18
77.53	8
84.35	11
84.90	14
86.21	12
89.76	13
89.92	9
91.73	5
97.53	7
97.75	15
106.00	3
114.80	4
145.60	1
153.40	6
165.10	2

These data show good correlation between high values of h_{FE_o} and early failure.

5.1.2 The h_{ie} Parameter

Figure 14 shows the normalized h_{ie} data for the group, exclusive of three unusual specimens which are shown in Figure 15. The normalized h_{ie} curve follows the general pattern of the normalized h_{FE} curve (Figure 12). The similarity of the two

curves may be explained by relationship:

$$h_{ie} = r_b + (h_{fe} + 1)\, r_e$$

where r_b = base spreading resistance, and

r_e = emitter junction resistance.

Since $h_{fe} \approx h_{FE}$ the expression may be written:

$$h_{ie} \approx r_b + (h_{FE} + 1)\, r_e .$$

Normally $(h_{FE} + 1)\, r_e$ is the predominant factor and thus controls h_{ie}.

The fact that normalized h_{ie} (Figure 14) decreases more rapidly than normalized h_{FE} (Figure 12) indicates that either r_b or r_e, or both, may have been changed by the irradiation.

5.1.3 The I_{CBO} Parameter

The data shown in Figure 16 were all obtained at zero radiation rates before and after the test and at various reactor shutdown periods during the test. No data are shown for periods when the reactor was operating because changes in I_{CBO} at these times were masked by radiation rate effects in the instrumentation cables. These effects have been measured previously and are known to be approximately 0.40 μA at 35 V for a reactor rate of 3 megawatts without shielding. Since the system for measuring I_{CBO} had a maximum sensitivity of 10^{-8} A and an accuracy of $\pm$ 10 nA, small changes were masked by cable effects.

A portion of the increase in I_{CBO} indicated by the data point at 1.6×10^{15} n/cm^2 may have been due to the elevated temperature of the specimens (see Figure 8).

5.2 TYPE TI 551 DIODE

Twenty (20) specimens manufactured by Texas Instruments were tested. The specimens were irradiated in an environmental chamber adjusted to maintain the temperature at $30^{\circ} \pm 2^{\circ}$ C. However, gamma heating near the end of the test caused the temperature to rise above the specified limits. Figure 9 shows the temperature trace for these specimens.

One of the specimens was unusual in that its pre-test values of V_F and I_R were much above those of the other nineteen specimens. The data for this specimen were processed separately from those of the other specimens.

5.2.1 The V_F Parameter

The behavior of the V_F parameter for the group is shown in Figure 17. There was a gradual decline of the median V_F until about 10^{14} n/cm^2. After that point it began a sharp rise.

None of the specimen failed because of an increase in V_F by a factor of two. However, the trend of the median at the end of the test indicated that the median failure point (100% increase in V_F) would have been about 3×10^{15} n/cm^2 had the irradiation been continued. Post-test readings, taken three days after the end of the test indicated some annealing of the radiation damage to the V_F parameter.

Figure 18 shows the V_F parameter for the one unusual specimen. This specimen showed a gradual increase in V_F until about 10^{13} n/cm^2 then a more rapid rise. The post test measurements showed a value of V_F lower than the pre-test value.

5.2.2 The I_R Parameter

Figure 19 portrays the I_R data for the TI 551 group. The median I_R remained less

than 0.1 μA until about 10^{14} n/cm^2, then it began to rise. A portion of this rise was a radiation rate effect as evidenced by decreases in I_R immediately after reactor shutdowns at about 6.5×10^{14} n/cm^2 and at the end of the test. There was also a further decrease in I_R during the 66-hour period between the end of the test and the taking of final measurements.

In regard to the I_R parameter failure of a specimen was defined as an increase in I_R above 0.2 μA. Using this criteria all specimens failed during the test. The pattern of failure is shown in Figure 20. A portion of the I_R increase during the latter part of the test was undoubtedly due to temperature increase (see Figure 9).

Figure 21 shows the I_R data for the one unusual specimen.

5.3 THERMISTORS

Nine groups of five specimens each were tested. The specimens were mounted on four circuit boards and potted. The boards were immersed in ice baths in two Dewar flasks, two boards in each flask. The flasks were then inserted into a block of styrofoam. Specimen types placed in each of the Dewar flasks were as follows:

DEWAR NO. 1

No.	Type	Manufacturer
5	A0610P-13	Carborundum
5	A1406P-13	Carborundum
5	R172	General Electric
5	GB31L1	Fenwal
5	GB41L1	Fenwal

DEWAR NO. 2

No.	Type	Manufacturer
5	RL13M1	Keystone
5	RL20E1	Keystone
5	RL4M1	Keystone
5	RL7E1	Keystone

The baths could not be maintained at a constant temperature during the irradiation due to gamma heating. Bath temperatures were monitored by copper-constantan thermocouples which gave readings believed accurate to $\pm 2^{\circ}$ C. These bath temperatures are shown in Figures 10 and 11 and also in Figures 22 through 39.

The temperatures as indicated by the thermistor specimens during the test, and after the test, are shown in Figures 22 through 39. These temperatures were calculated assuming all specimens were indicating the bath temperature (0° C) in the pre-test measurement.

Note in the even-numbered figures (large ordinate scale) that at reactor rate number 7 (3 megawatts without the LiH shield) the specimen temperatures generally rose faster than the bath temperature. This is believed to be due to gamma heating of the specimen, or the potting compound, while the bath still contained ice. On the other hand, in the odd-numbered figures at the same reactor rate, but after the bath ice had melted, the specimen temperatures generally lagged the bath temperature.

Note also in the even-numbered figures that the measurements taken at zero radiation rate (rate number 4) show lower temperatures than those taken immediately before at rate number 7.

Because of the uncertainty concerning the true bath temperature after the ice had melted, it is difficult to draw any conclusion from these data. However, during the short period at reactor rate 7 before the ice melted, it appears that all of the specimens except two (specimens 2 and 5, Figure 32) experienced some gamma heating.

An indication of the permanent effect of the radiation on the specimens can be seen from a tabulation of the temperatures indicated by the specimens in an ice bath approximately 66 hours after the end of the irradiation:

TYPE	MANUFACTURER	SPECIMEN NO.	TEMPERATURE ($^{\circ}$ C)
A0610P-13	Carborundum	1	-1.08
A0610P-13	Carborundum	2	-1.43
A0610P-13	Carborundum	3	-5.04
A0610P-13	Carborundum	4	-2.86
A0610P-13	Carborundum	5	-2.44
A1406P-13	Carborundum	1	-.01
A1406P-13	Carborundum	2	-.18
A1406P-13	Carborundum	3	-.06
A1406P-13	Carborundum	4	0
A1406P-13	Carborundum	5	-.12
R172	General Electric	1	-.90
R172	General Electric	2	-.81
R172	General Electric	3	+ .04
R172	General Electric	4	+ .07
R172	General Electric	5	+ .33

TYPE	MANUFACTURER	SPECIMEN NO.	TEMPERATURE (°C)
GB31L1	Fenwal	1	0
GB31L1	Fenwal	2	-.07
GB31L1	Fenwal	3	-.03
GB31L1	Fenwal	4	+.05
GB31L1	Fenwal	5	-.33
GB41L1	Fenwal	1	+4.96
GB41L1	Fenwal	2	+ .05
GB41L1	Fenwal	3	+ .11
GB41L1	Fenwal	4	+ .06
GB41L1	Fenwal	5	+ .15
RL13M1	Keystone	1	+ .16
RL13M1	Keystone	2	+ .39
RL13M1	Keystone	3	-.01
RL13M1	Keystone	4	+ .09
RL13M1	Keystone	5	+ .06
RL20E1	Keystone	1	+ .04
RL20E1	Keystone	2	+ .04
RL20E1	Keystone	3	+ .05
RL20E1	Keystone	4	+2.04
RL20E1	Keystone	5	+3.00
RL4M1	Keystone	1	+ .11
RL4M1	Keystone	2	-.20
RL4M1	Keystone	3	+ .12
RL4M1	Keystone	4	+ .05
RL4M1	Keystone	5	+ .05
RL7E1	Keystone	1	+ .08
RL7E1	Keystone	2	-.02

TYPE	MANUFACTURER	SPECIMEN NO.	TEMPERATURE ($^{\circ}$ C)
RL7E1	Keystone	3	-.15
RL7E1	Keystone	4	-.02
RL7E1	Keystone	5	+ .03

From these data it would appear that the A0610P-13 type does show a permanent radiation effect. No other group contained specimens which all showed a permanent effect, although individual specimens of the types R172, GB41L1, and RL20E1 showed permanent damage.

TABLE 1 TEST SPECIMENS AND TEST CONDITIONS

Board No.	Description	No. Tested	Test Conditions	Parameter
1	Transistor 2N2501, NPN, Si General Instrument	20	V_{CB} = 35 V, I_E = 0 V_{CE} = 10 V, I_C = 10 mA V_{CE} = 5 V, I_C = 1 mA, I_{SIG} = 10 μA at 1 kc	I_{CBO} h_{FE} h_{ie}
2	Diode TI 551 Texas Instruments	20	I_F = 100 mA V_R = 200 V	V_F I_R
3 and 4	Thermistor A0610P-13 Carborundum	5	Power = 0.8 MW T = 0° C	Resistance
3	Thermistor A1406P-13 Carborundum	5	Power = 1.2 MW T = 0° C	Resistance
3	Thermistor R172 General Electric	5	Power = 1.65 MW T = 0° C	Resistance
4	Thermistor GB31L1 Fenwal	5	Power = 0.07 MW T = 0° C	Resistance
4	Thermistor GB41L1 Fenwal	5	Power = 0.07 MW T = 0° C	Resistance
5	Thermistor RL13M1 Keystone	5	Power = 2.0 MW T = 0° C	Resistance
5	Thermistor RL20E1 Keystone	5	Power = 0.29 MW T = 0° C	Resistance
6	Thermistor RL4M1 Keystone	5	Power = 2.0 MW T = 0° C	Resistance
6	Thermistor RL7E1 Keystone	5	Power = 0.29 MW T = 0° C	Resistance

TABLE 2 MANUFACTURERS' SPECIFICATIONS FOR TEST SPECIMENS

Test Specimen	Specifications				
Transistor 2N2501	h_{FE} = 50 - 150 At V_{CE} = 10 V and I_C = 10 mA I_{CBO} = .025 μA At V_{CB} = 40 V				
Diode TI 551	V_F = 1.0 V At I_F = 100 mA, T = 25° C I_R = .10 μA At V_R = 225V, T = 25° C				
Thermistors	Resistance At 25° C	Tolerance At 25° C	Resistance At 0° C	Dissipation Constant MW/° C	Maximum Temperature (° C)
A0610P-13	2000 Ω	± 20%	500 Ω	8	125
A1406P-13	250 Ω	± 20%	62.5 Ω	12	125
R172	5000 Ω	± 10%	14,500 Ω	16.5	145
GB31L1	1000 Ω	± 20%	2900 Ω	0.7	300
GB41L1	10,000 Ω	± 20%	29,000 Ω	0.7	300
RL13M1	90.8 Ω	± 10%*	312.5 Ω	20	150
RL20E1	9090 Ω	± 10%*	33,180 Ω	2.9	150
RL4M1	20.85 Ω	± 10%*	61.44 Ω	20	150
RL7E1	1005 Ω	± 10%*	3156 Ω	2.9	150

*At 37.8° C

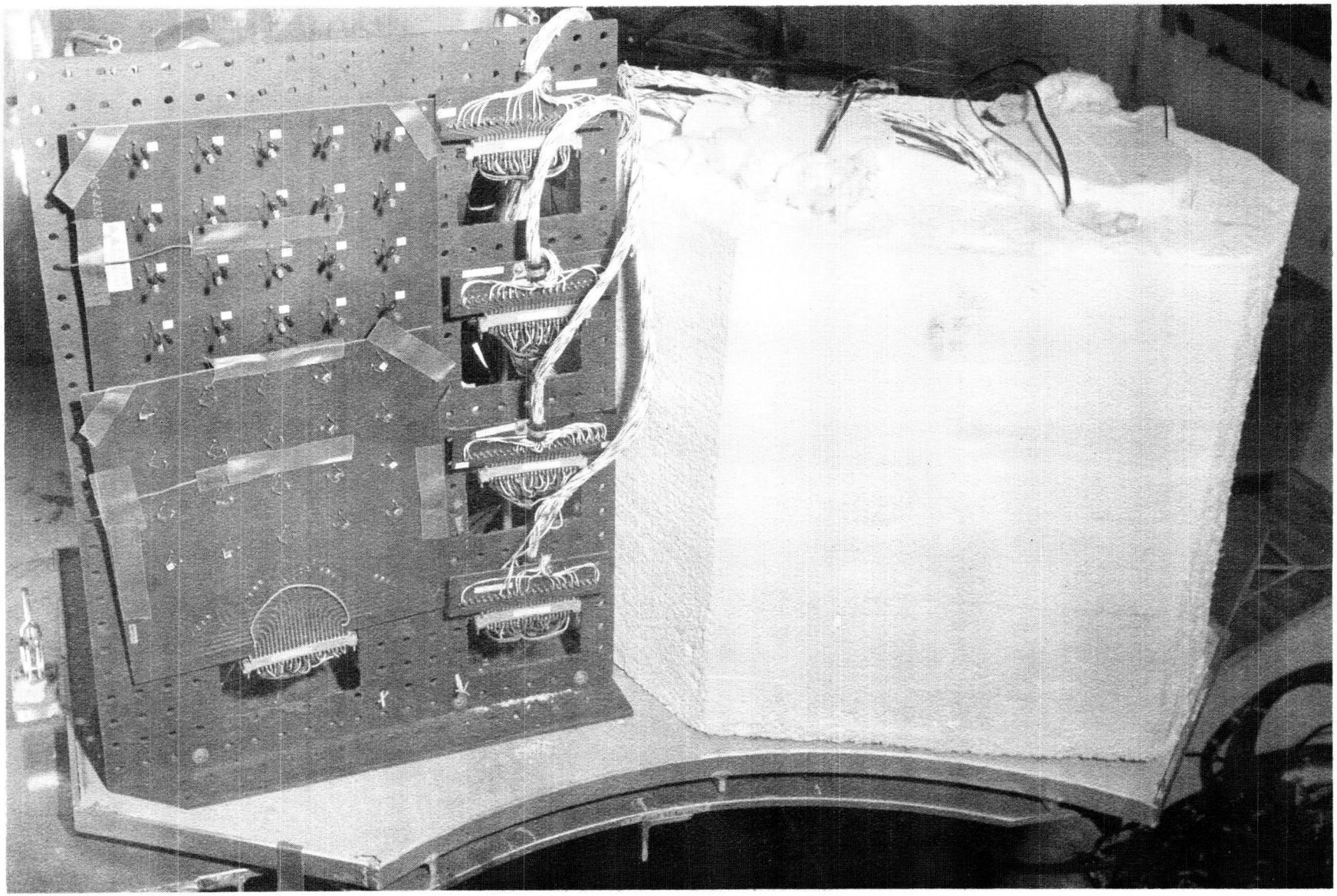

FIGURE 1 TEST PANEL AND DEWAR INSULATING BLOCK AS SEEN FROM REACTOR

FIGURE 2 THERMISTOR BOARDS REMOVED FROM DEWARS

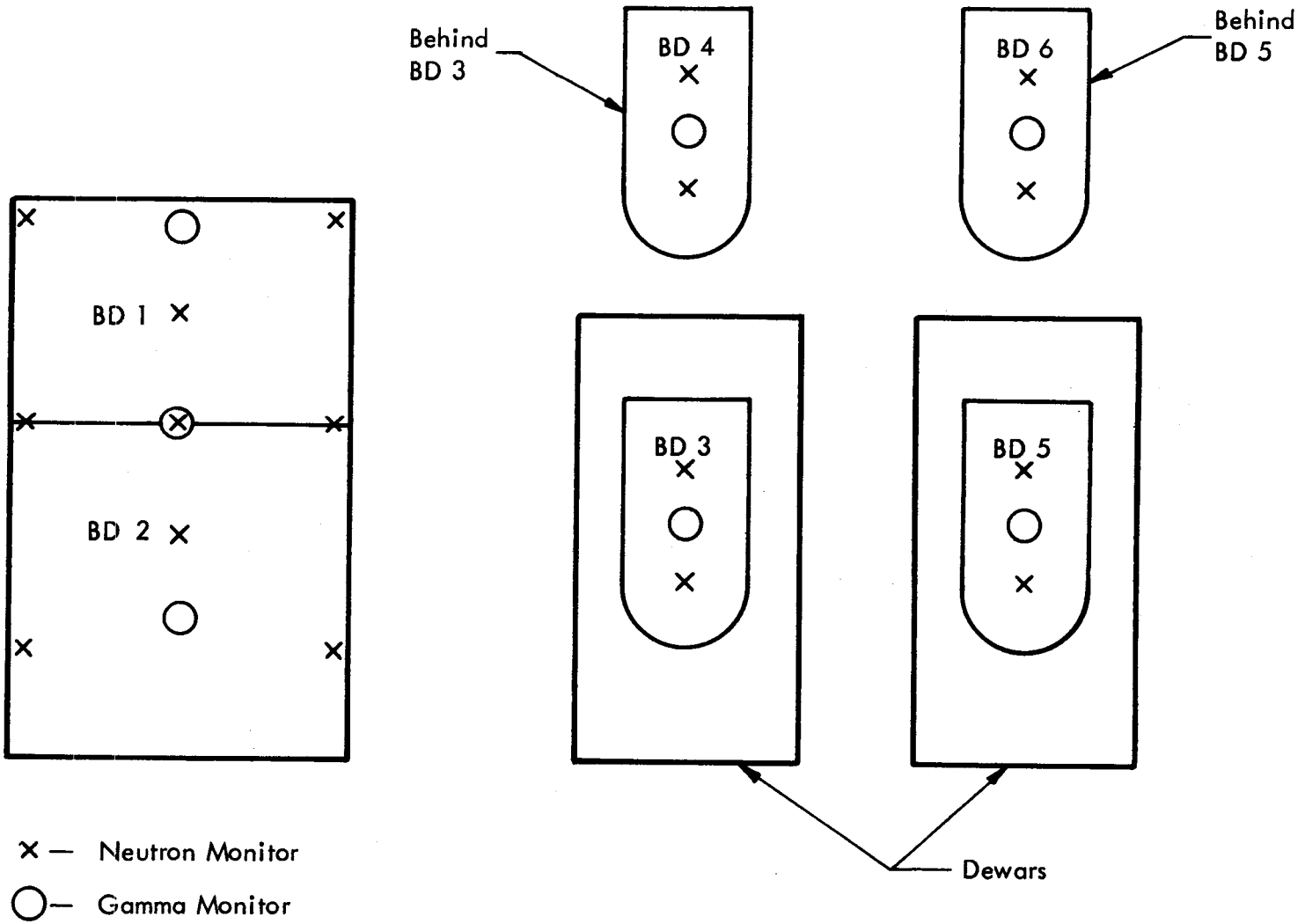

FIGURE 3 DIAGRAM OF TEST BOARDS AS SEEN FROM REACTOR

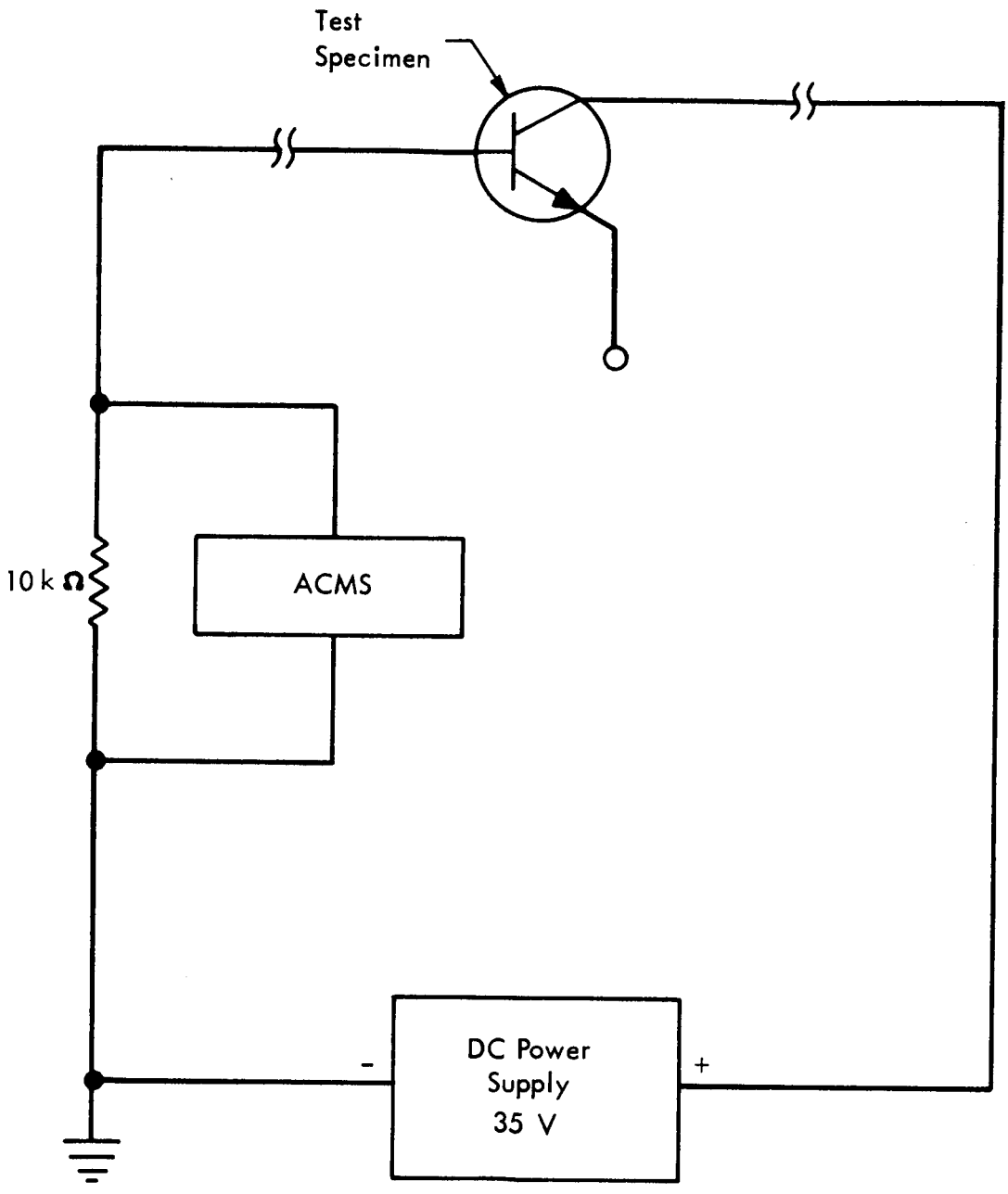

FIGURE 4 I_{CBO} MEASURING CIRCUIT

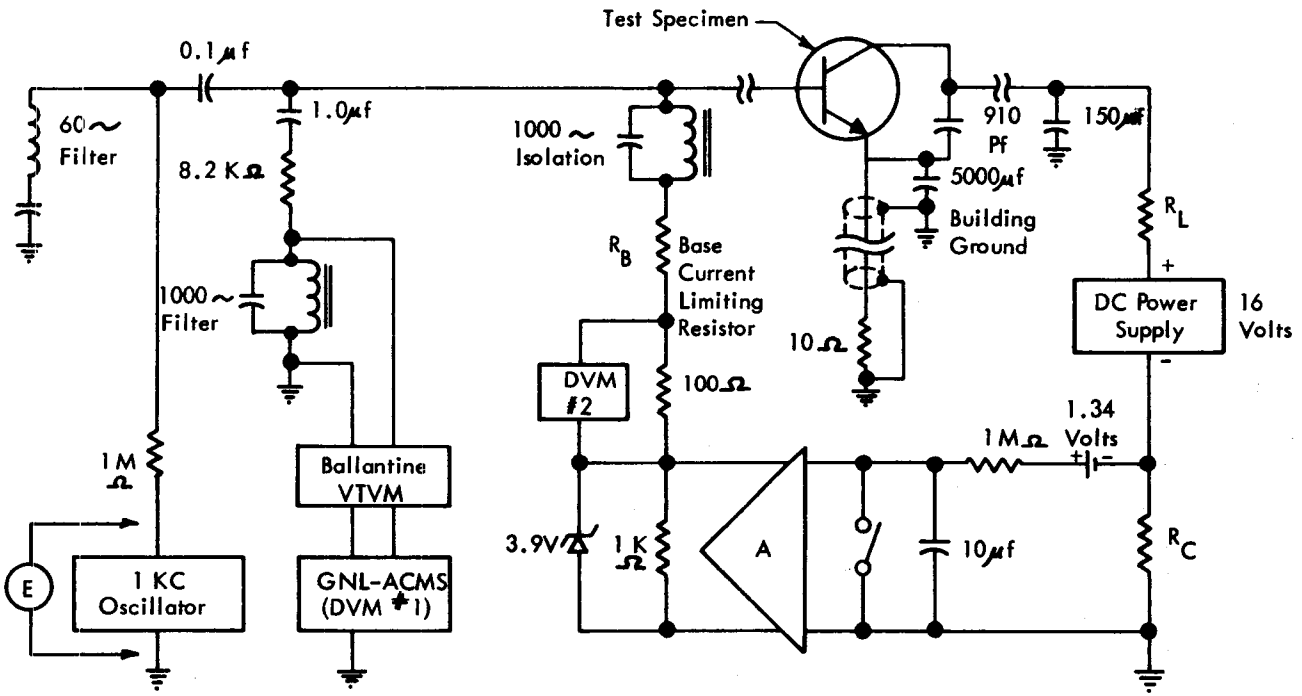

Measurement	I_C (ma)	R_L (ohm)	R_C (ohm)	R_B (ohm)	V_{CE}	E
h_{FE}	10	470	134	290	10	0
h_{ie}	1	9.7K	1.3K	3.9K	5	*

*AC Signal 10 μA

FIGURE 5 h_{FE} AND h_{ie} MEASURING CIRCUIT

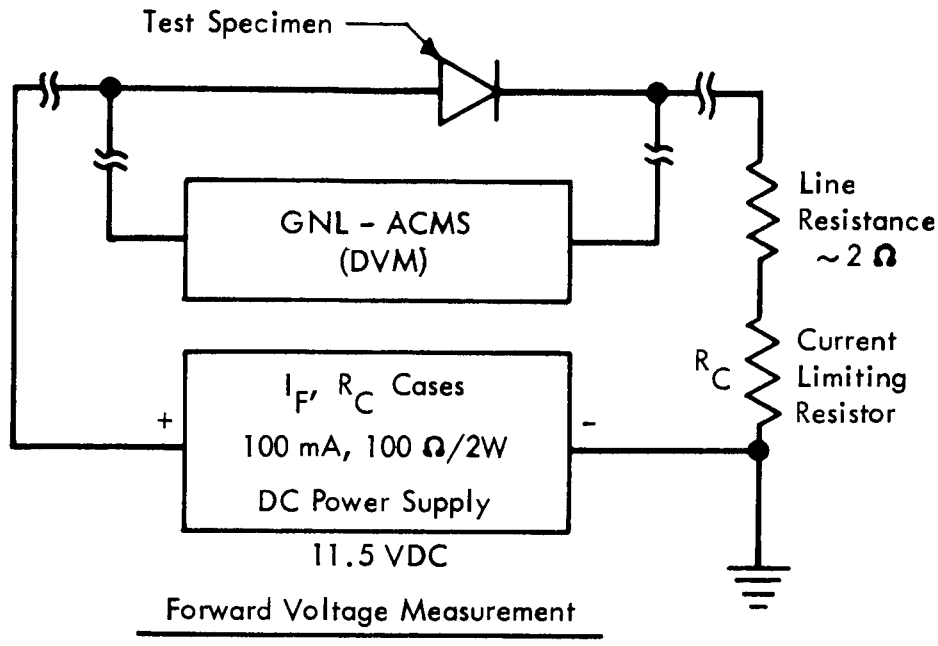

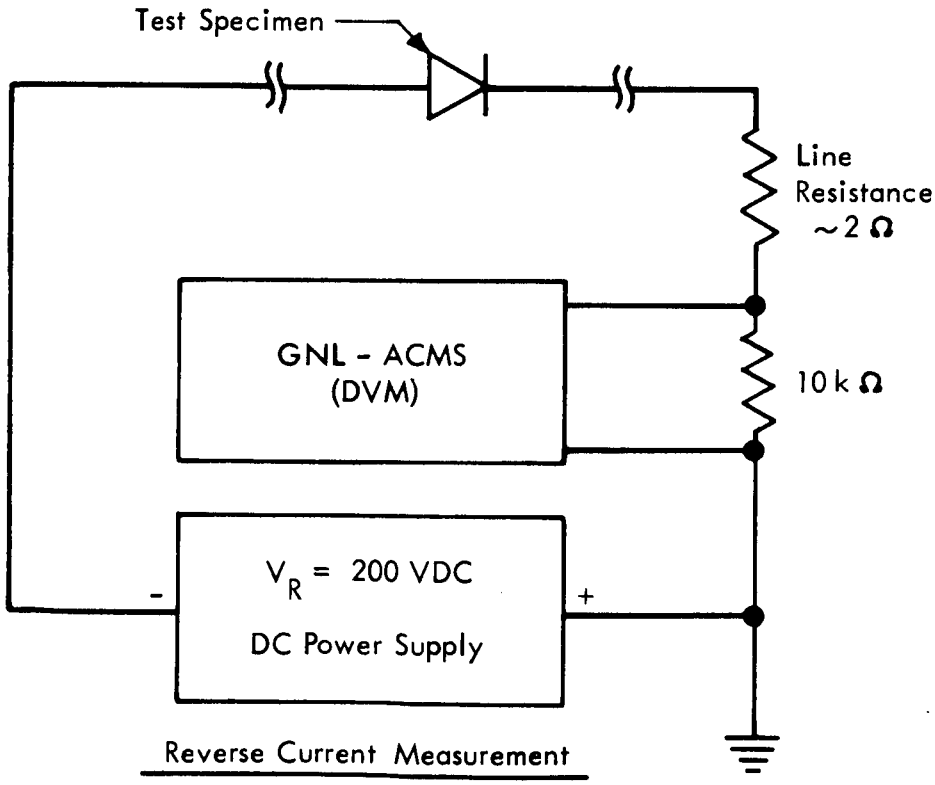

FIGURE 6 DIODE MEASURING CIRCUITS

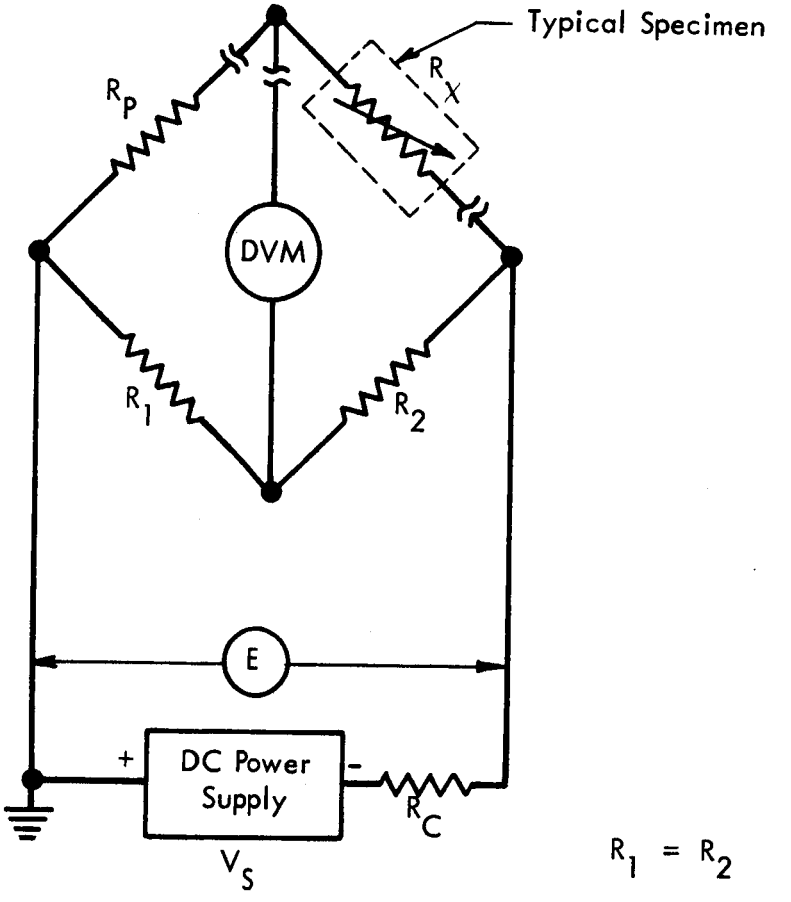

$R_1 = R_2$

$R_P \approx R_X$ at 0°C

Thermistor Type	V_S (VDC)	R_C (ohm)	R_P (ohm)	R_1 & R_2 (ohm)
G. E. R 172	200	570 k	15 k	150 k
Carborundum A0610P	10	16 k	500	75 k
Carborundum A1406P	10	5 k	65	75 k
Fenwal GB 31L1	10	60 k	2.9 k	75 k
Fenwal GB 41L1	80	740 k	29 k	150 k
Keystone RL 7E1	30	96 k	3.2 k	75 k
Keystone RL 20E1	50	500 k	33 k	150 k
Keystone RL 4M1	20	4 k	60	75 k
Keystone RL 13M1	40	20 k	310	75 k

FIGURE 7 THERMISTOR MEASURING CIRCUITS

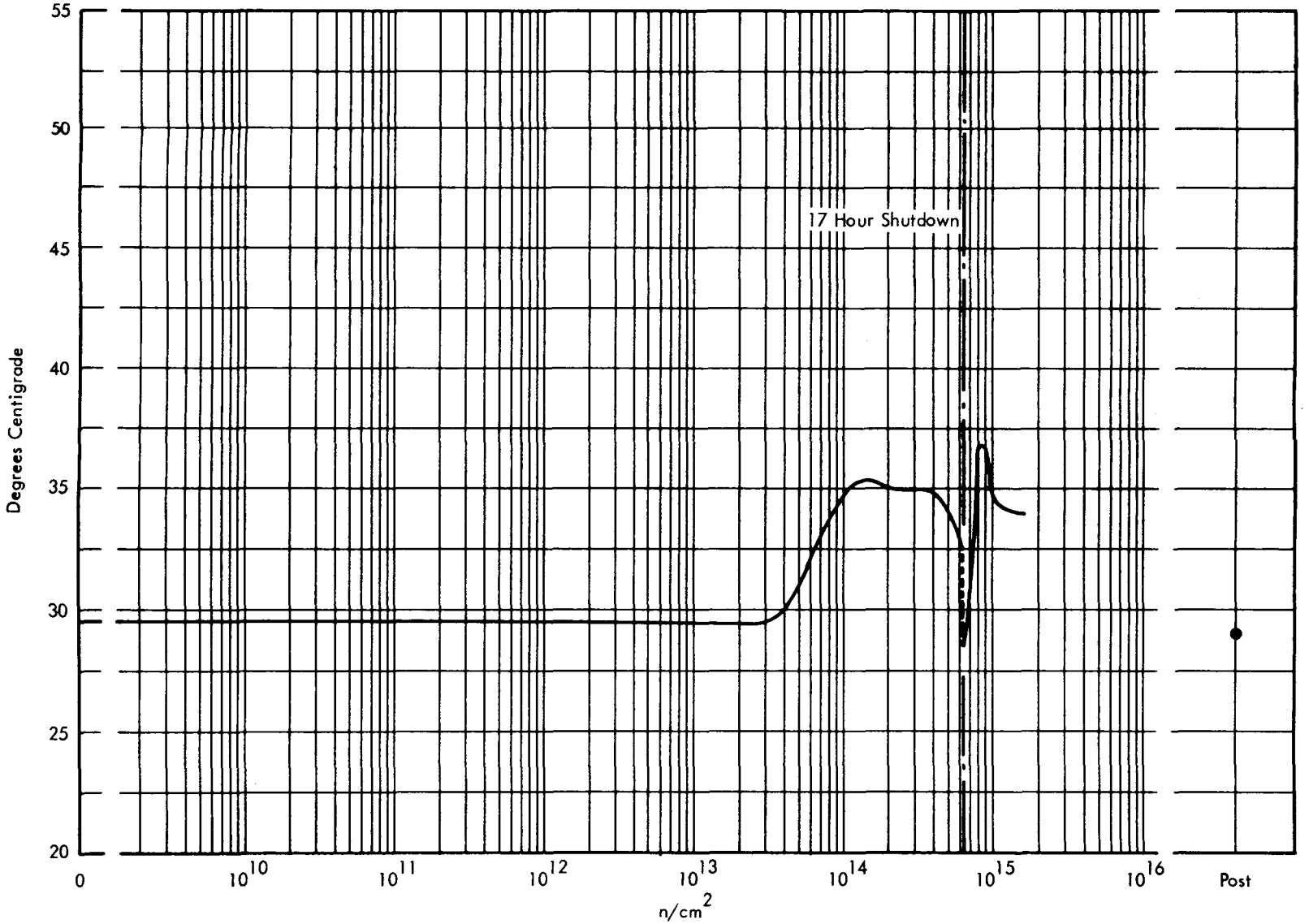

FIGURE 8 2N2501 TRANSISTORS, TEMPERATURE VERSUS INTEGRATED NEUTRON FLUX

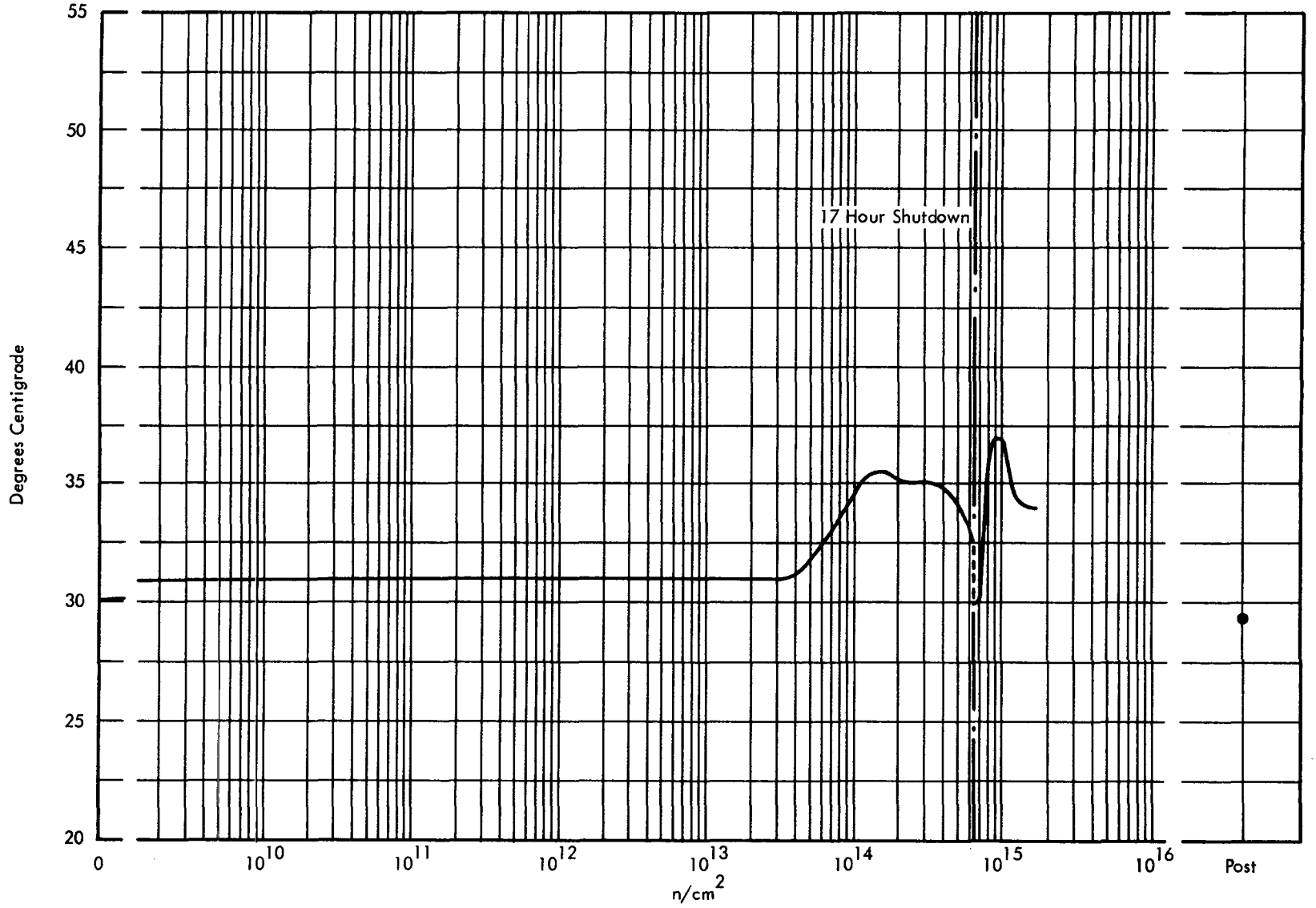

FIGURE 9 TI 551 DIODES, TEMPERATURE VERSUS INTEGRATED NEUTRON FLUX

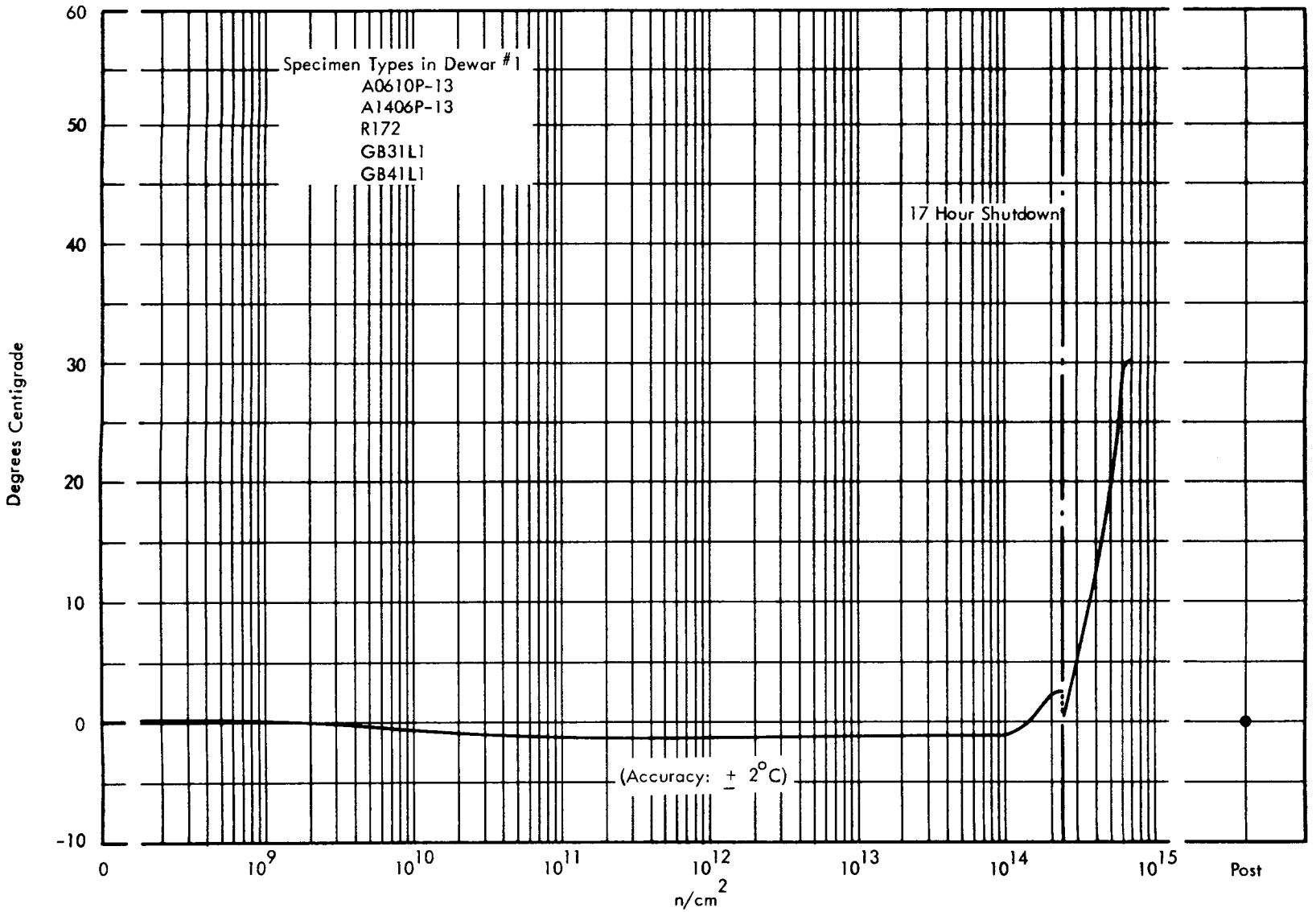

FIGURE 10 DEWAR NO. 1, BATH TEMPERATURE VERSUS INTEGRATED NEUTRON FLUX

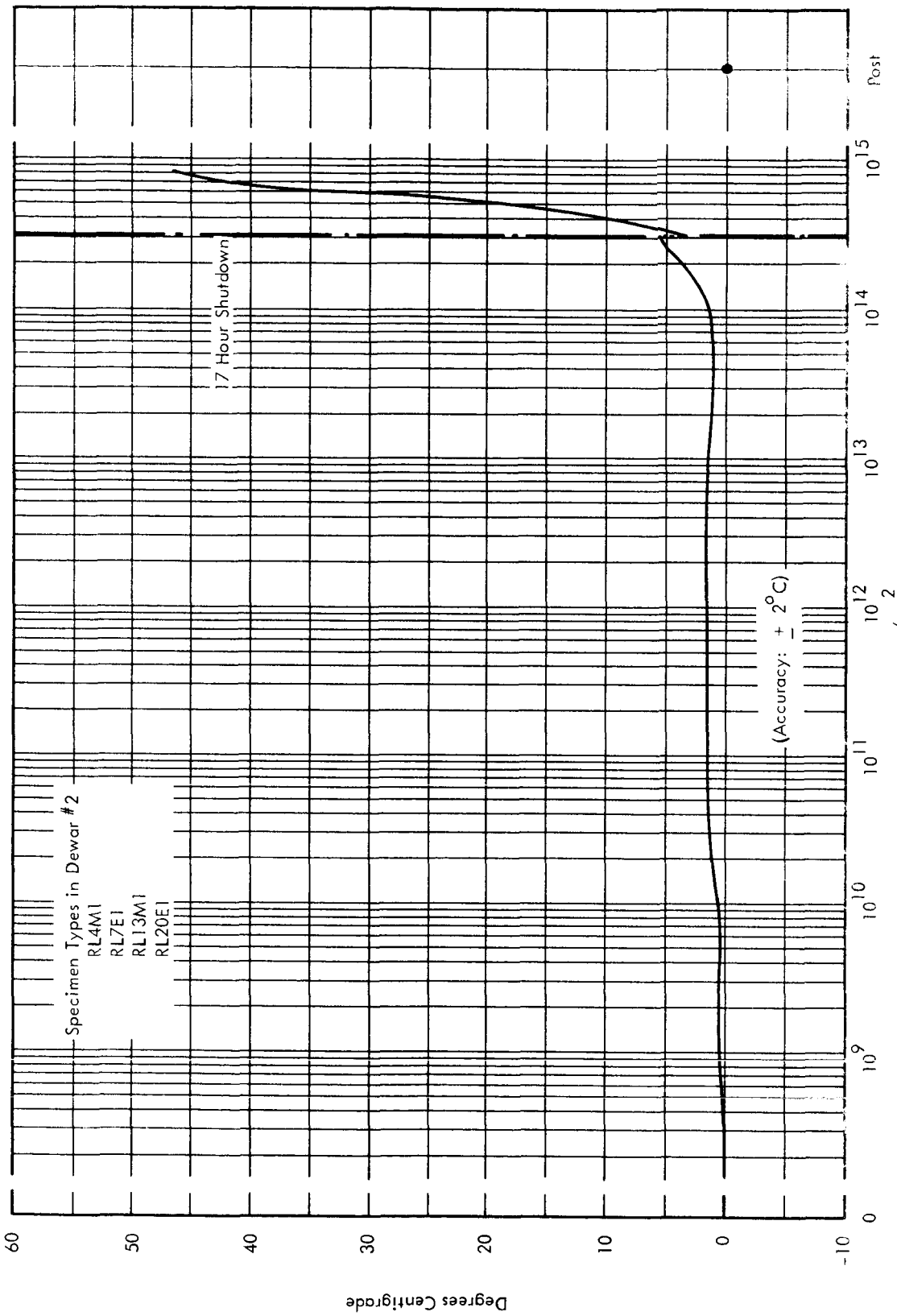

FIGURE 11 DEWAR NO. 2, BATH TEMPERATURE VERSUS INTEGRATED NEUTRON FLUX

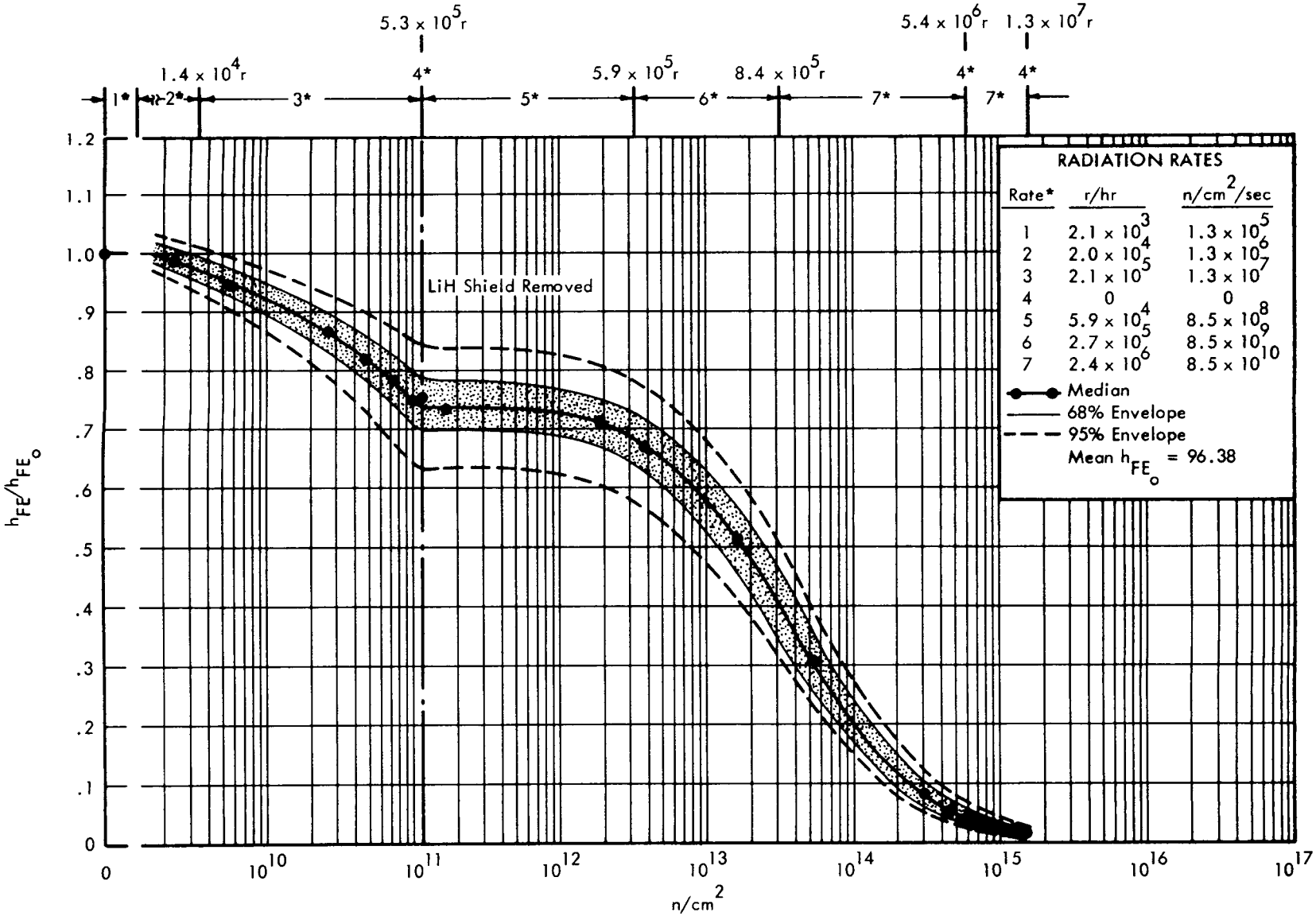

FIGURE 12 2N2501 GENERAL INSTRUMENT, 30°C, NORMALIZED h_{FE} VERSUS INTEGRATED NEUTRON FLUX

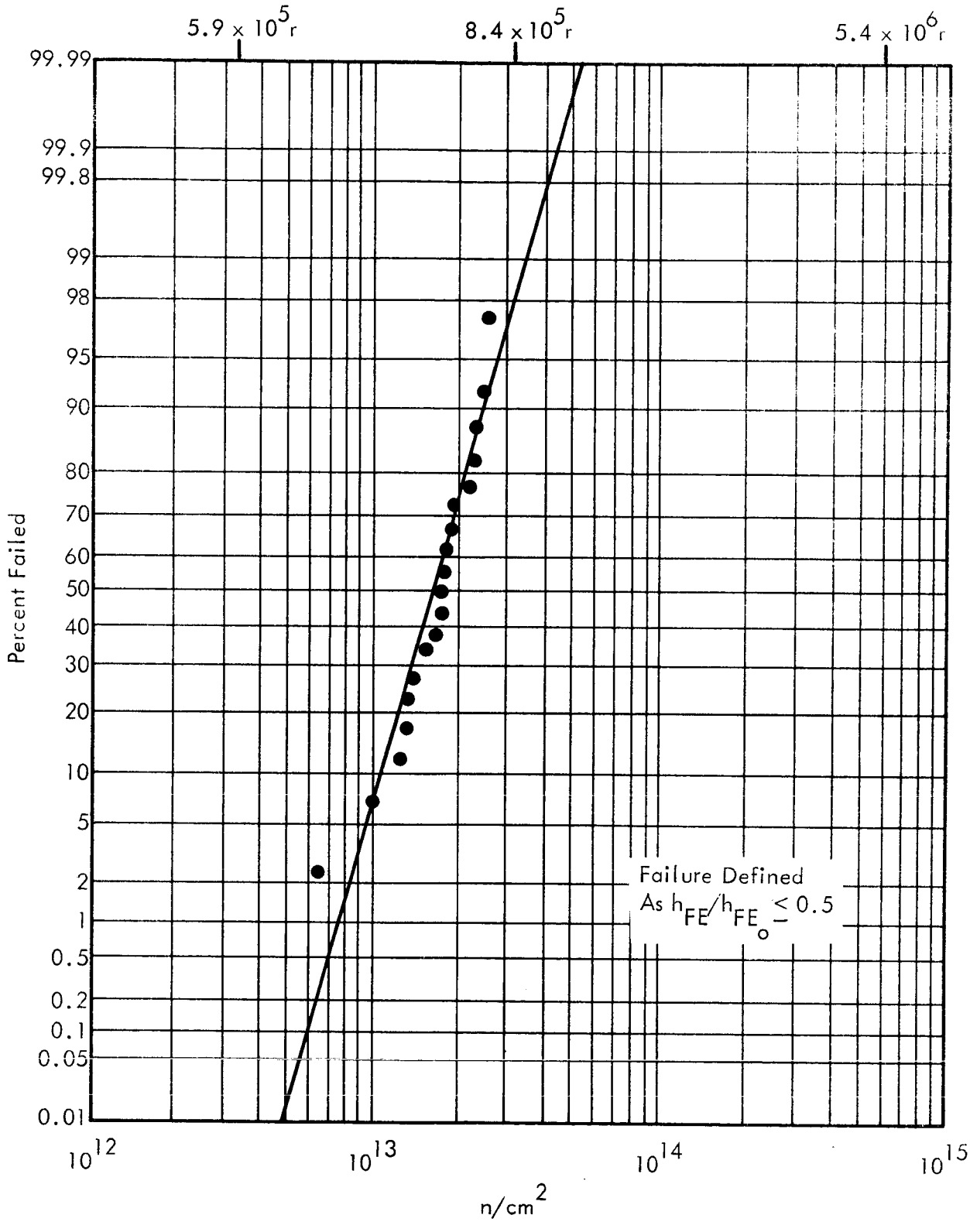

FIGURE 13 2N2501 GENERAL INSTRUMENT, 30°C, PERCENT FAILED VERSUS INTEGRATED NEUTRON FLUX

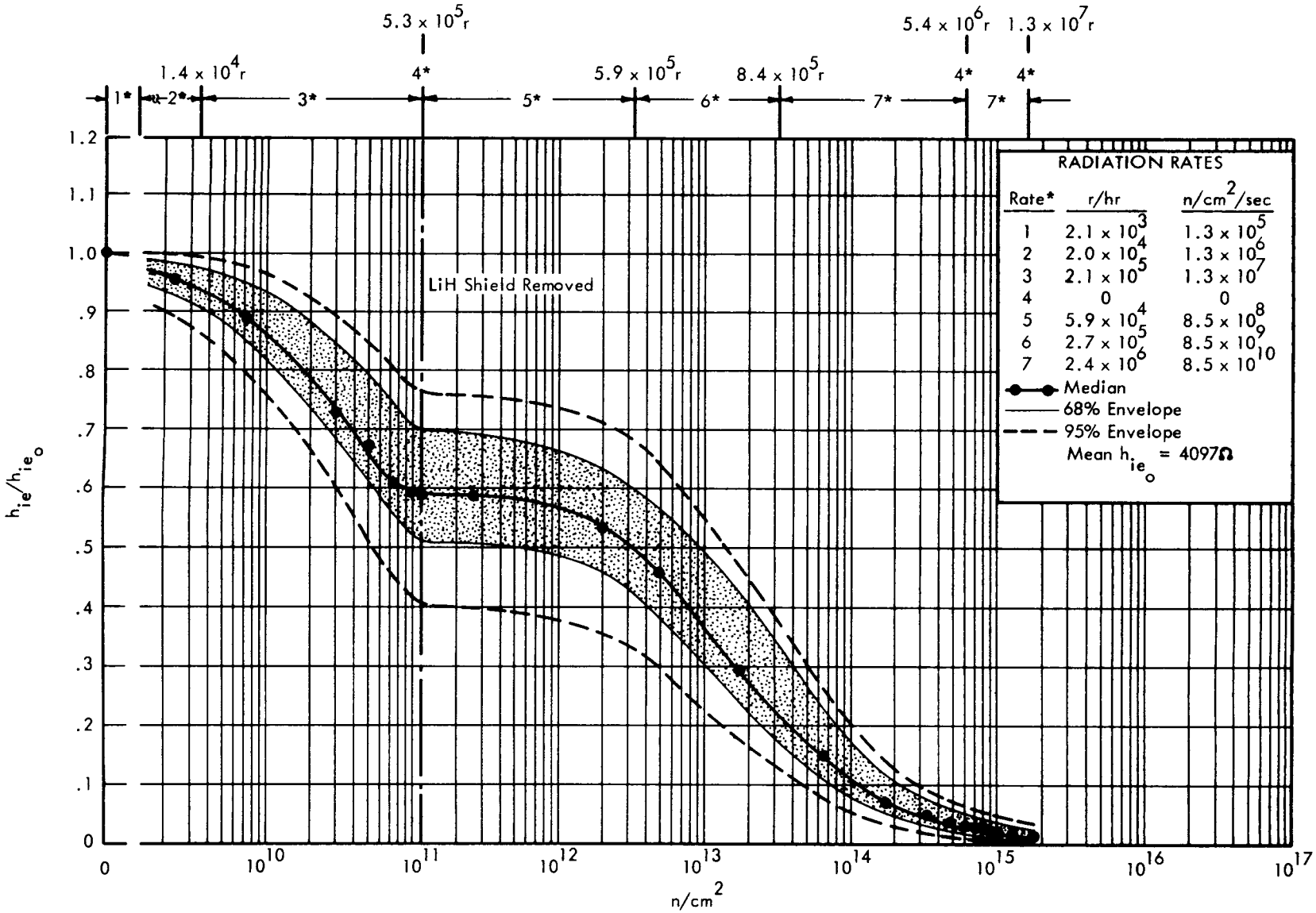

FIGURE 14 2N2501 GENERAL INSTRUMENT, 30°C, NORMALIZED h_{ie} VERSUS INTEGRATED NEUTRON FLUX

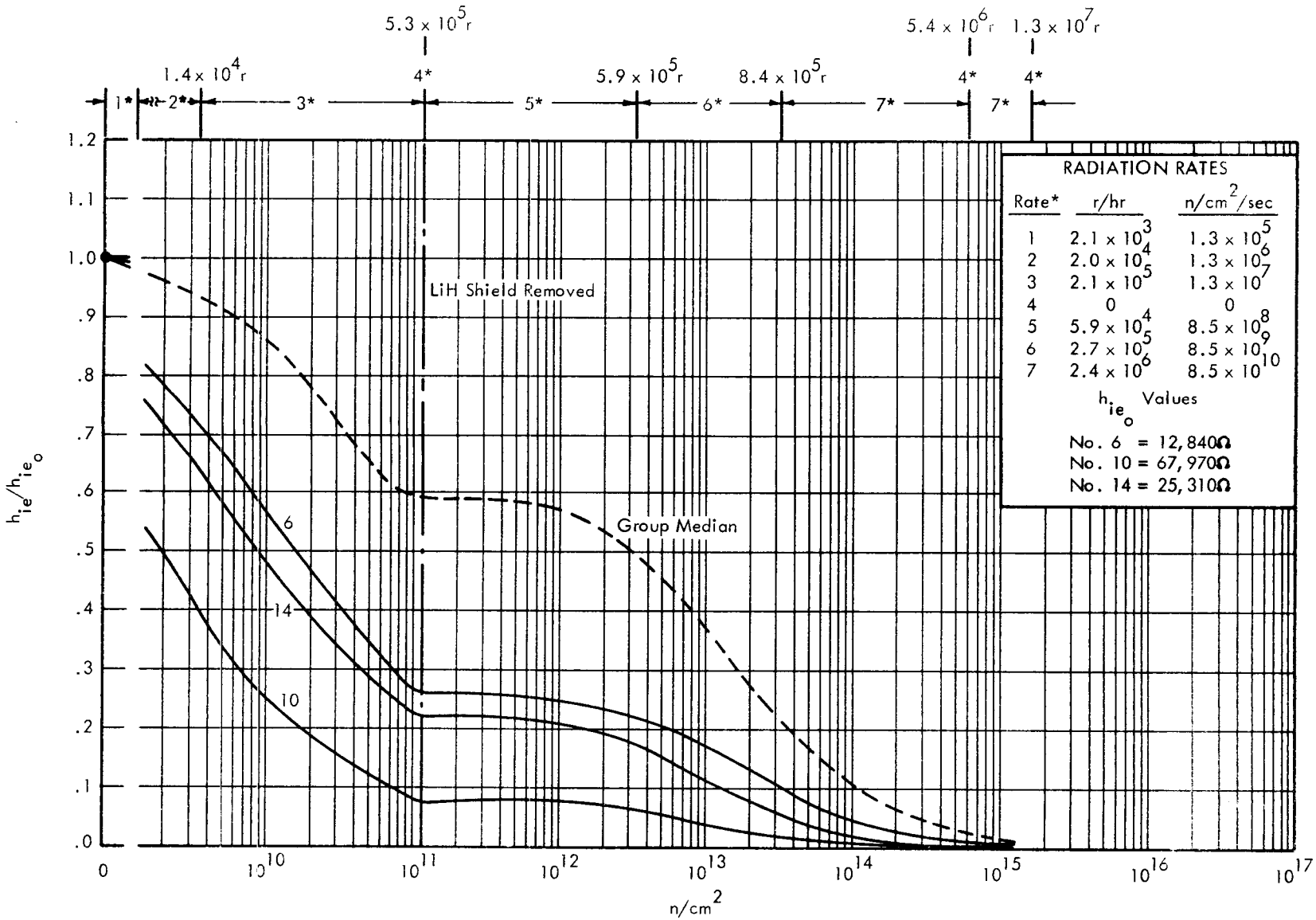

FIGURE 15 2N2501 GENERAL INSTRUMENT, (3 UNUSUAL SPECIMENS), 30°C, NORMALIZED h_{ie} VERSUS INTEGRATED NEUTRON FLUX

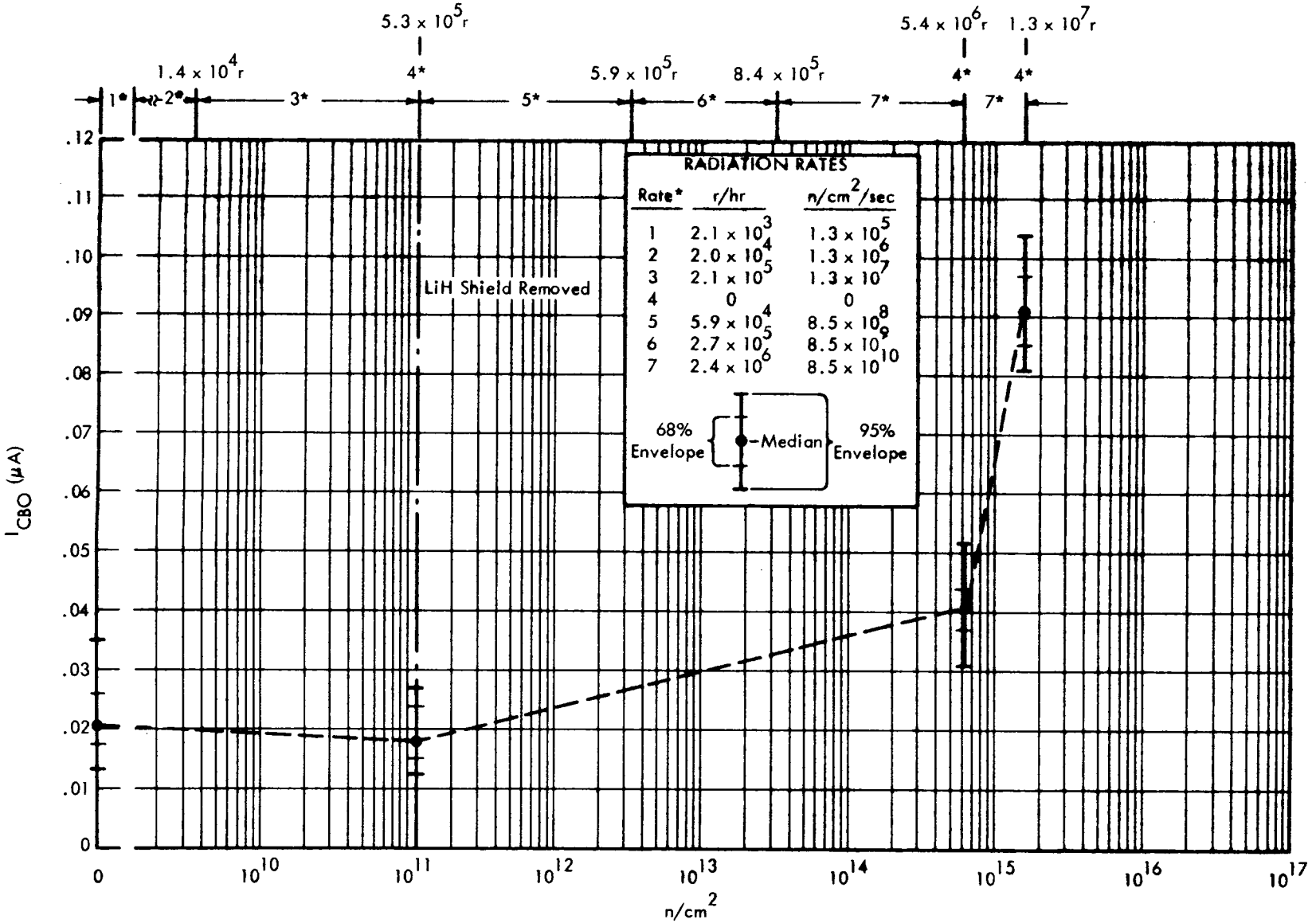

FIGURE 16 2N2501 GENERAL INSTRUMENT, 30°C, I_{CBO} VERSUS INTEGRATED NEUTRON FLUX

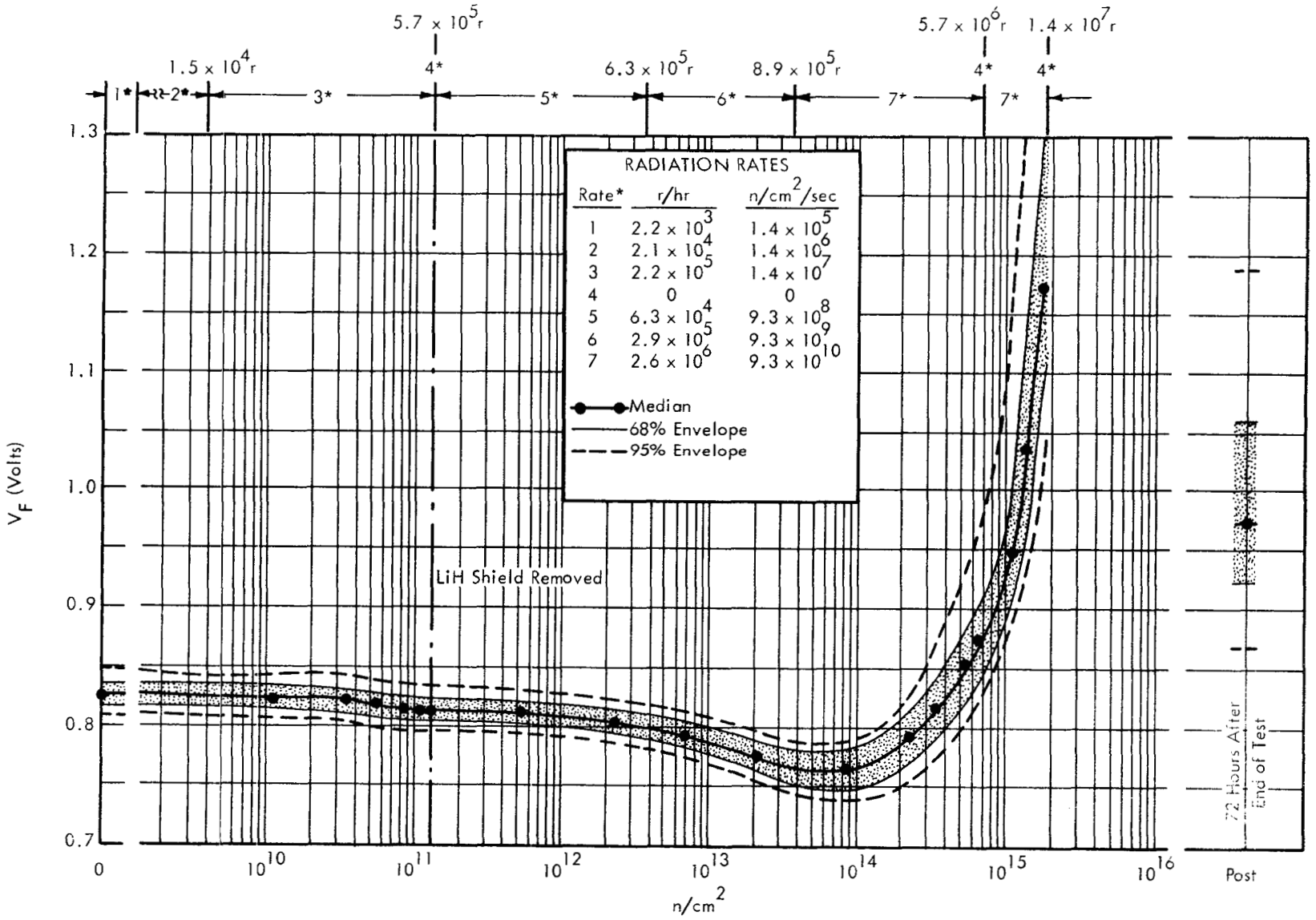

FIGURE 17 TI 551 TEXAS INSTRUMENTS, 30°C, V_F (I_F = 100mA) VERSUS INTEGRATED NEUTRON FLUX

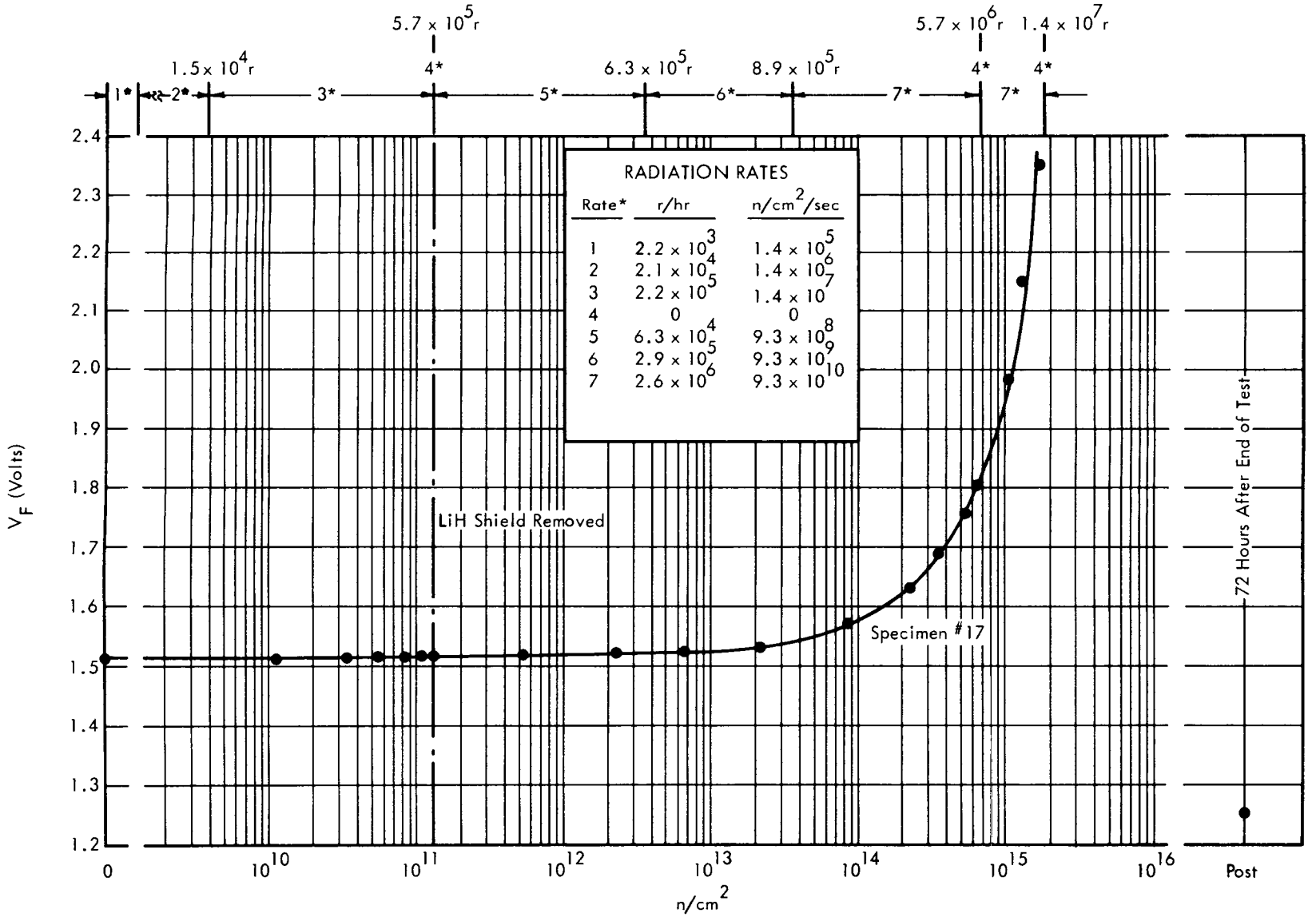

FIGURE 18 TI 551 TEXAS INSTRUMENTS (ONE UNUSUAL SPECIMEN), 30°C, V_F (I_F = 100mA) VERSUS INTEGRATED NEUTRON FLUX

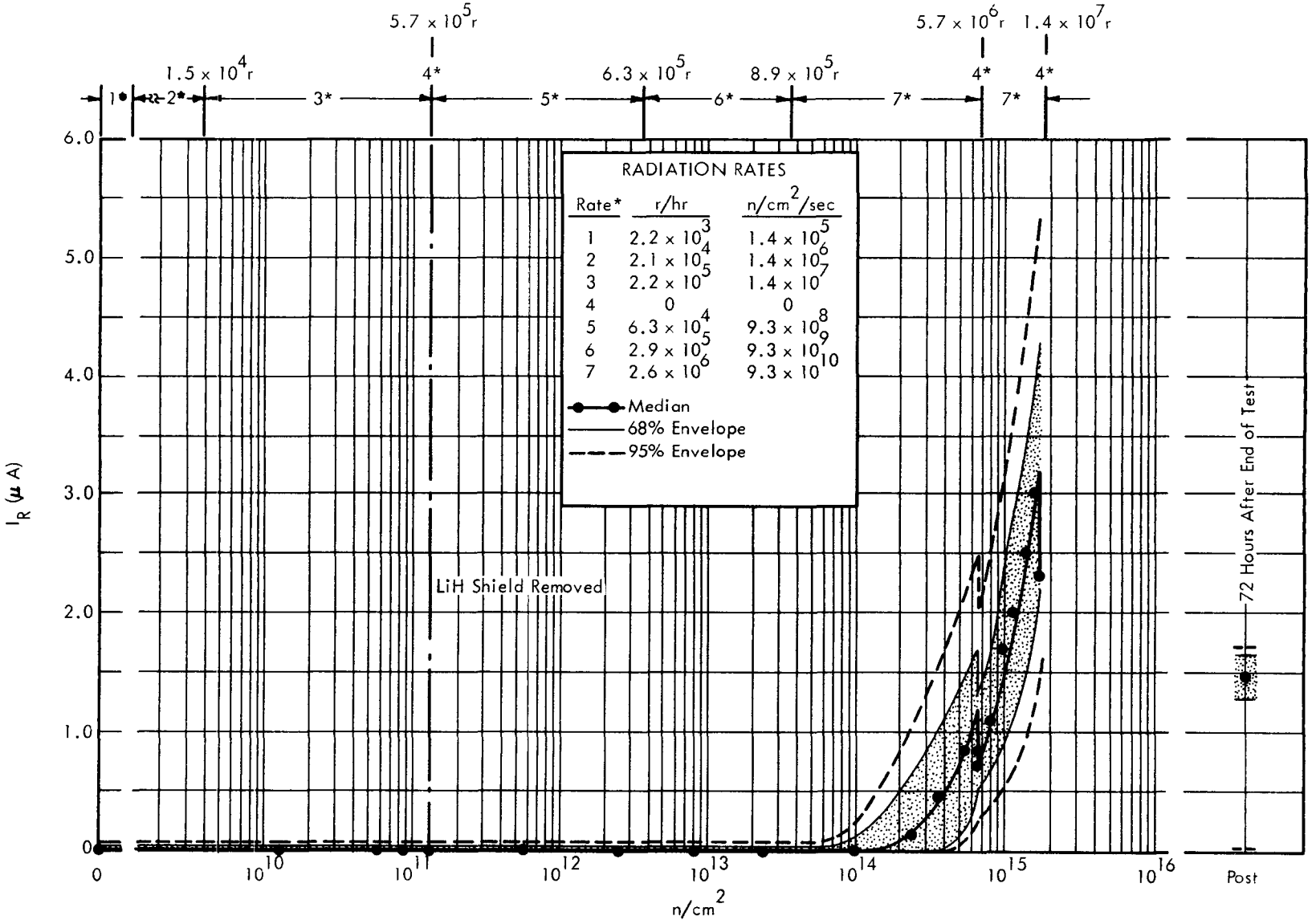

FIGURE 19 TI 551 TEXAS INSTRUMENTS, 30°C, I_R (V_R = 200V) VERSUS INTEGRATED NEUTRON FLUX

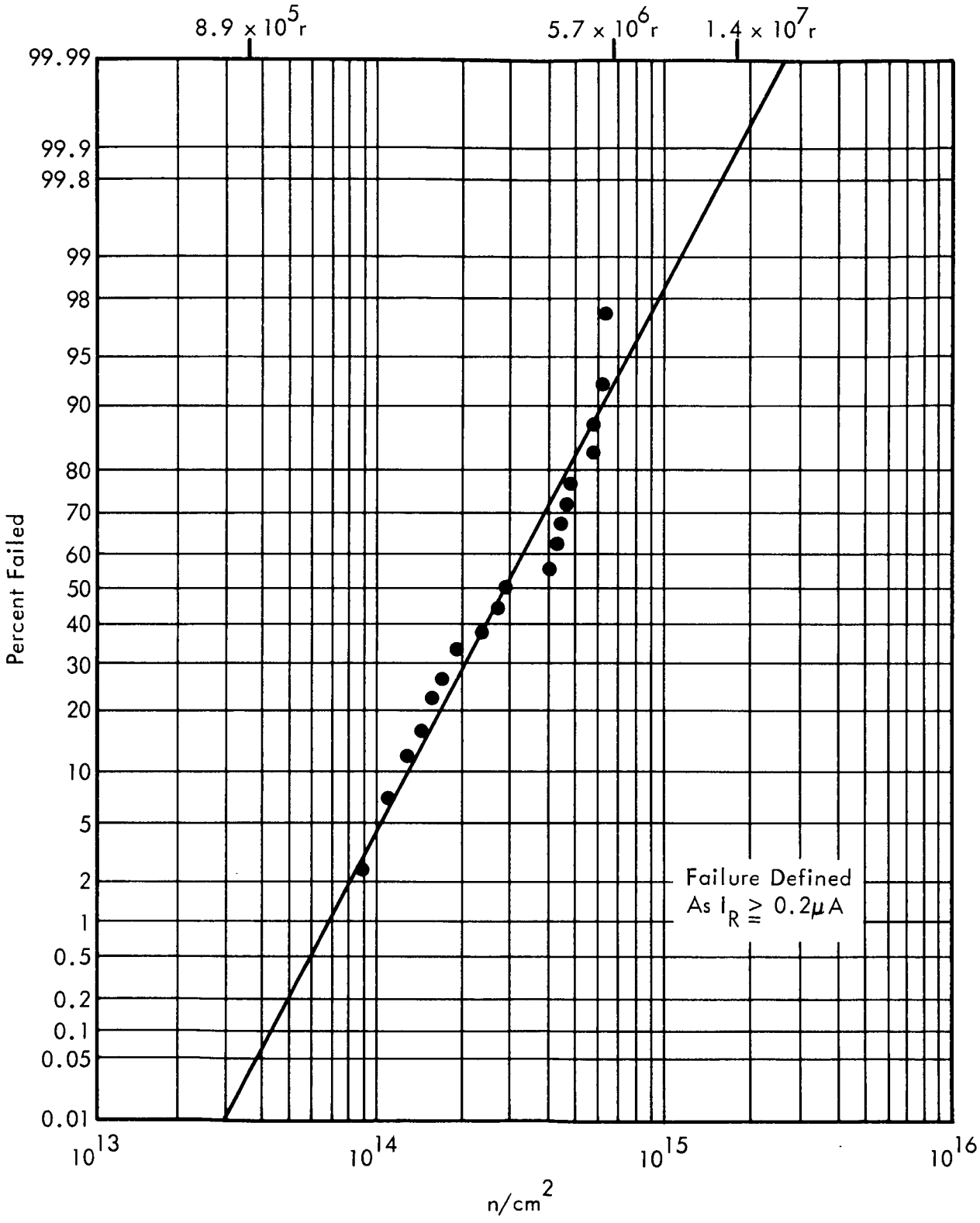

FIGURE 20 TI 551 TEXAS INSTRUMENTS, 30°C, PERCENT FAILED VERSUS INTEGRATED NEUTRON FLUX

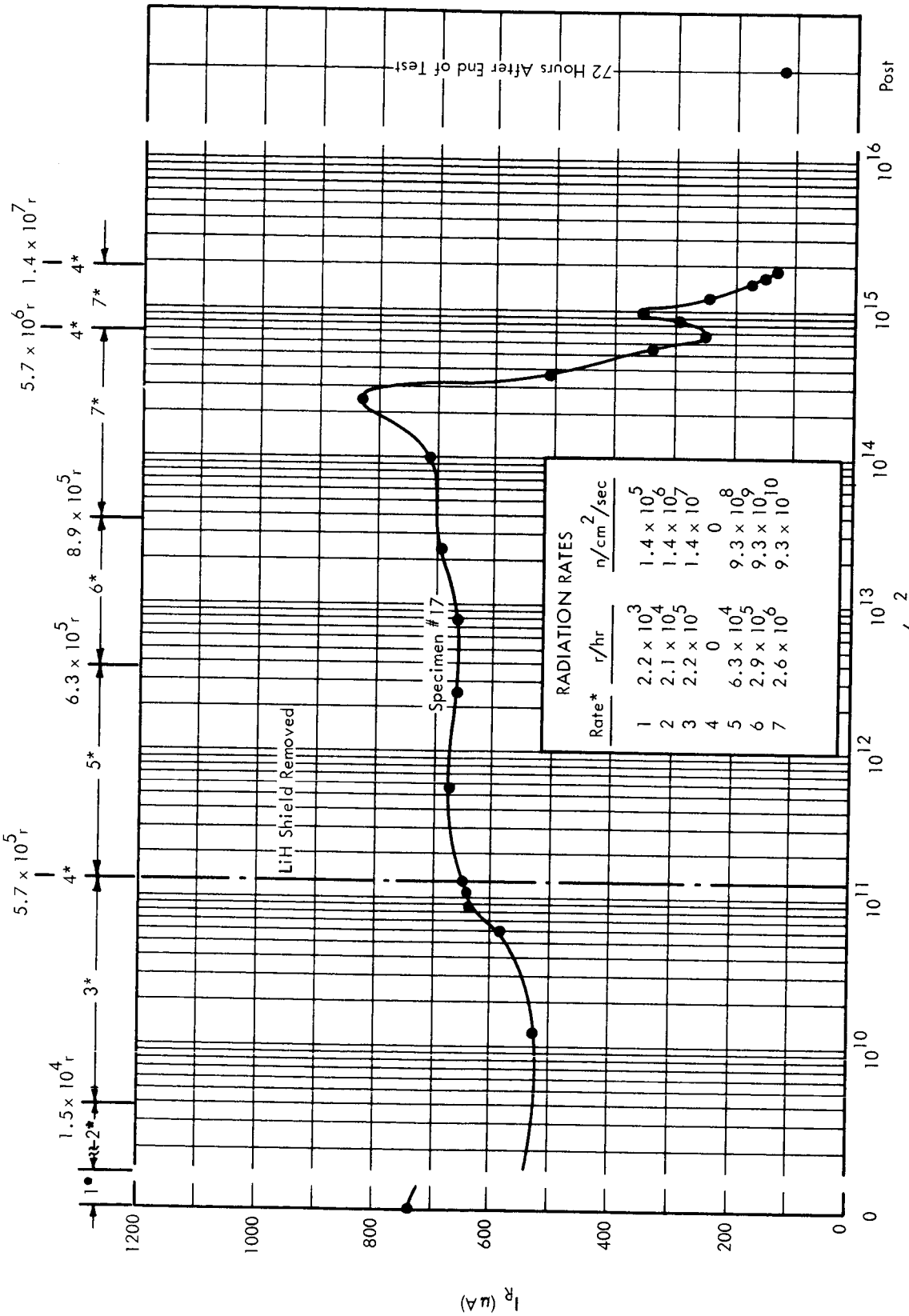

FIGURE 21 TI 551 TEXAS INSTRUMENTS (ONE UNUSUAL SPECIMEN), 30°C, I_R (V_R = 200V) VERSUS INTEGRATED NEUTRON FLUX

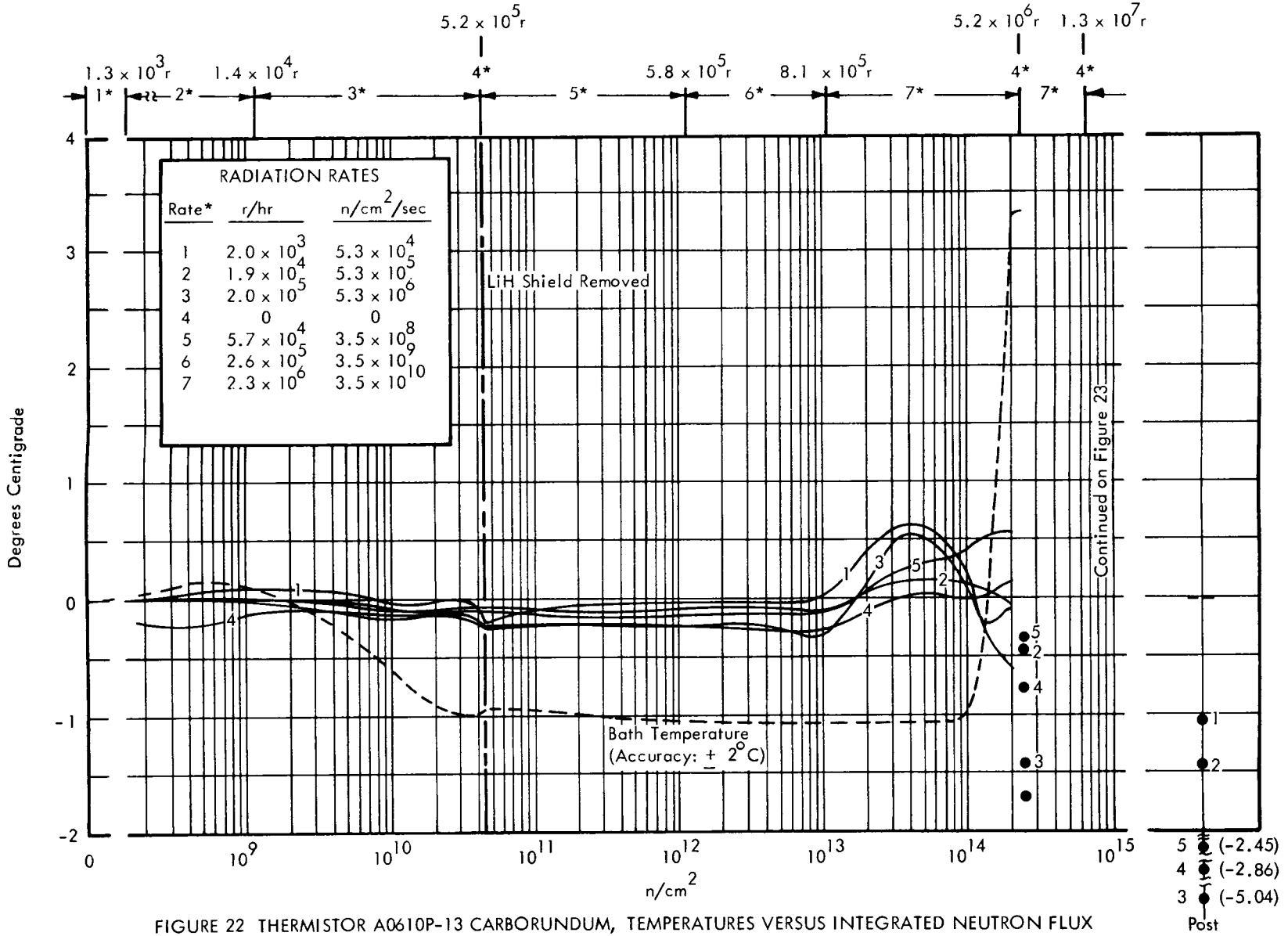

FIGURE 22 THERMISTOR A0610P-13 CARBORUNDUM, TEMPERATURES VERSUS INTEGRATED NEUTRON FLUX

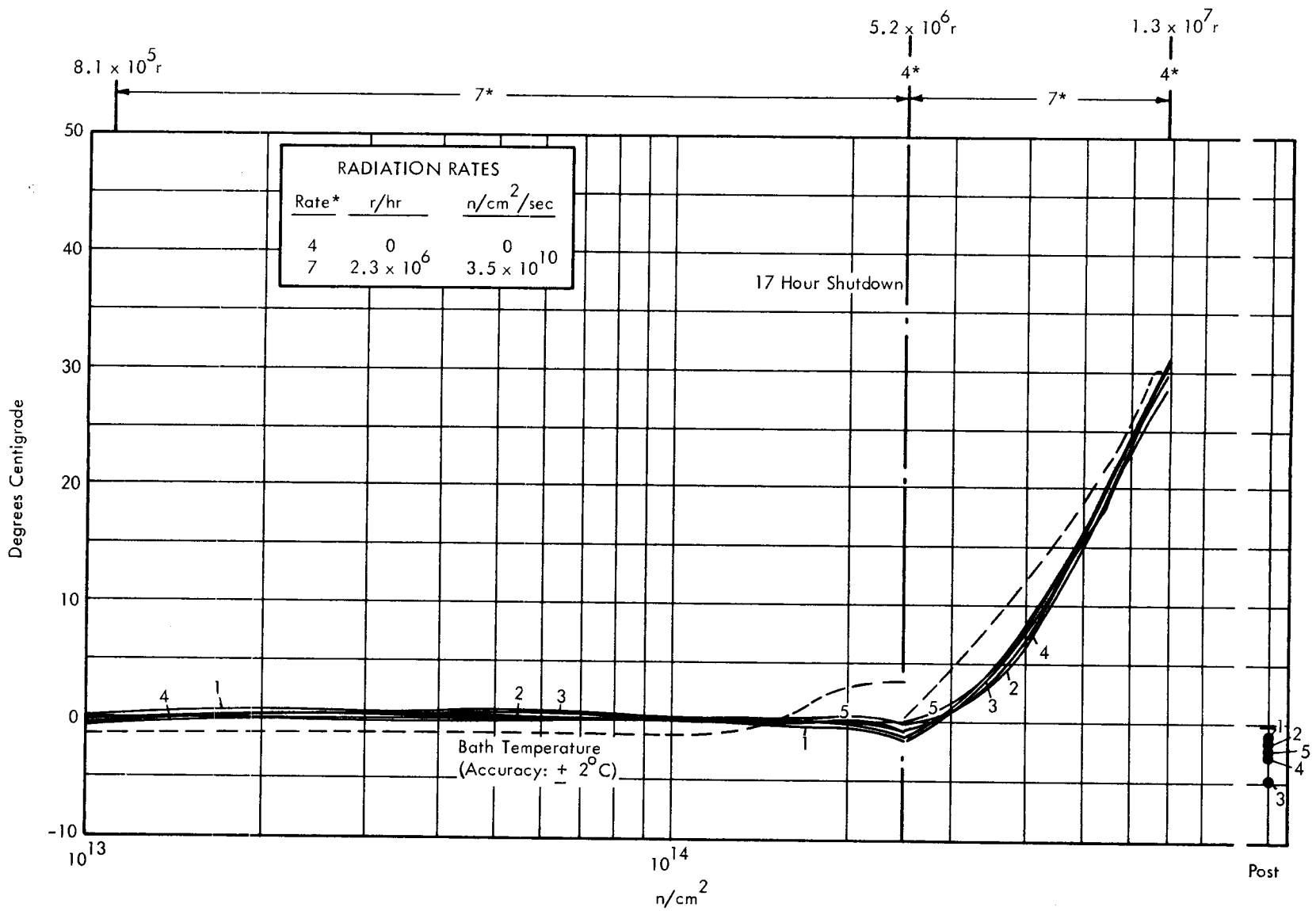

FIGURE 23 THERMISTOR A0610P-13 CARBORUNDUM, TEMPERATURES VERSUS INTEGRATED NEUTRON FLUX

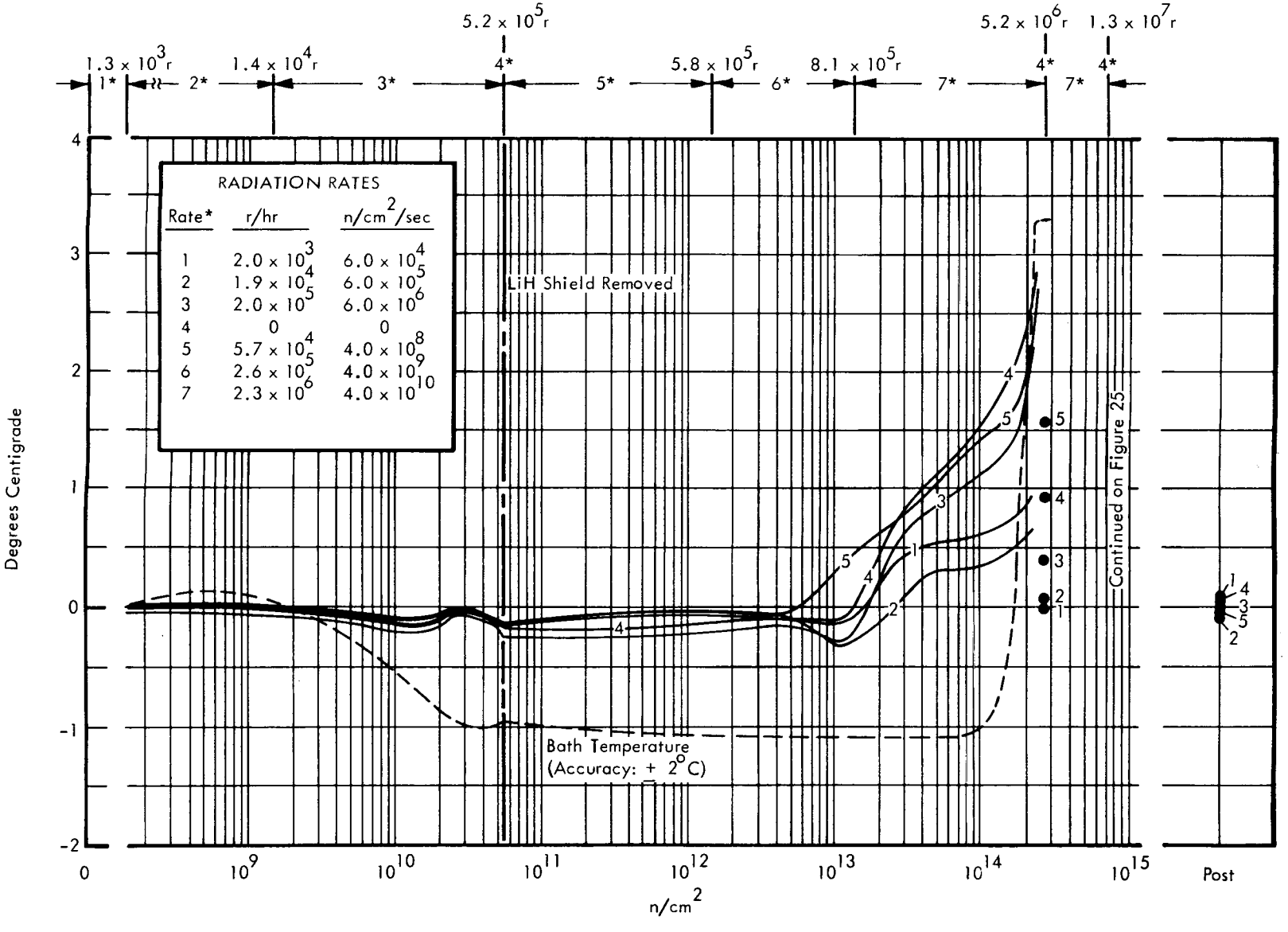

FIGURE 24 THERMISTOR A1406P-13 CARBORUNDUM, TEMPERATURES VERSUS INTEGRATED NEUTRON FLUX

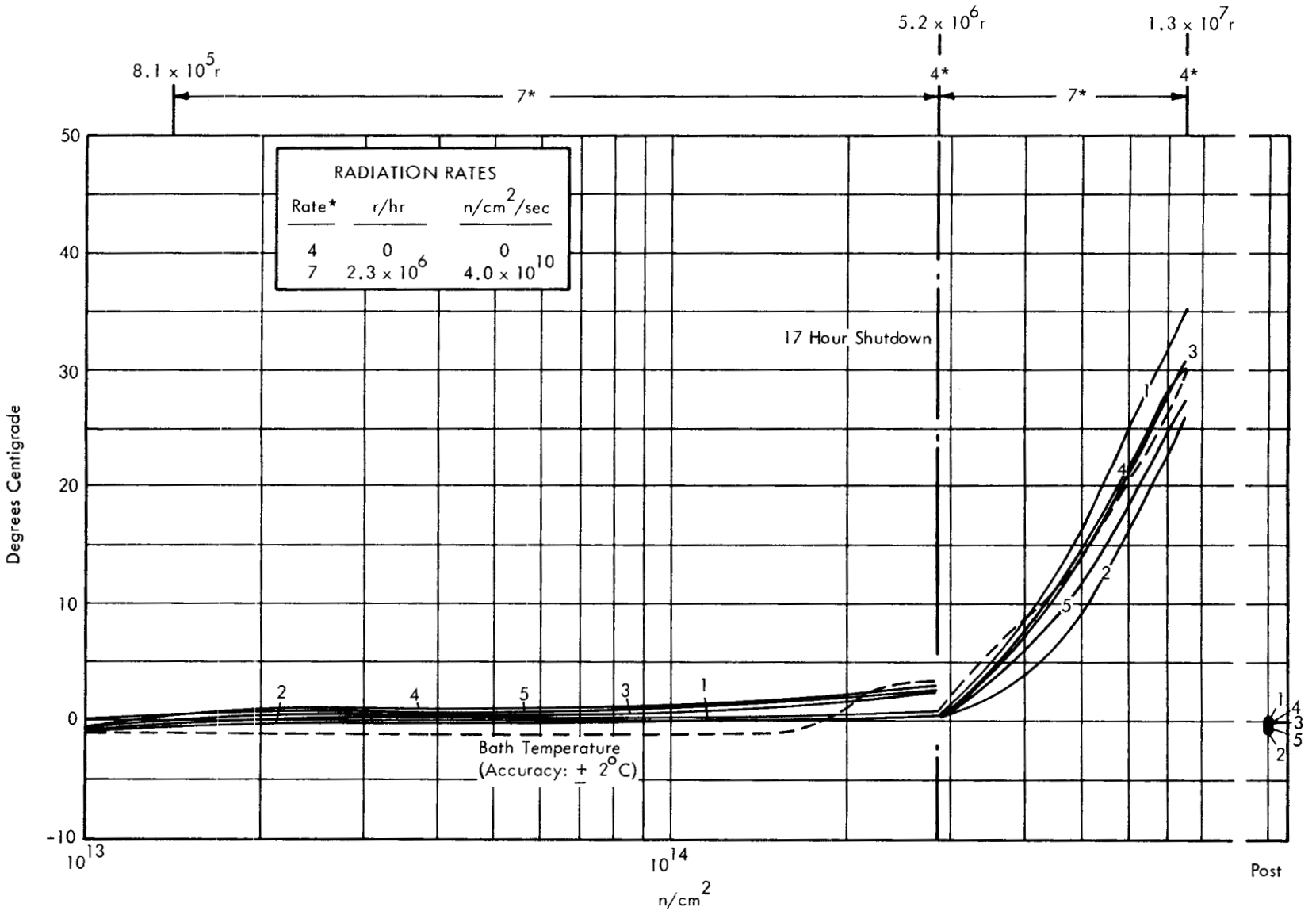

FIGURE 25 THERMISTOR A1406P-13 CARBORUNDUM, TEMPERATURES VERSUS INTEGRATED NEUTRON FLUX

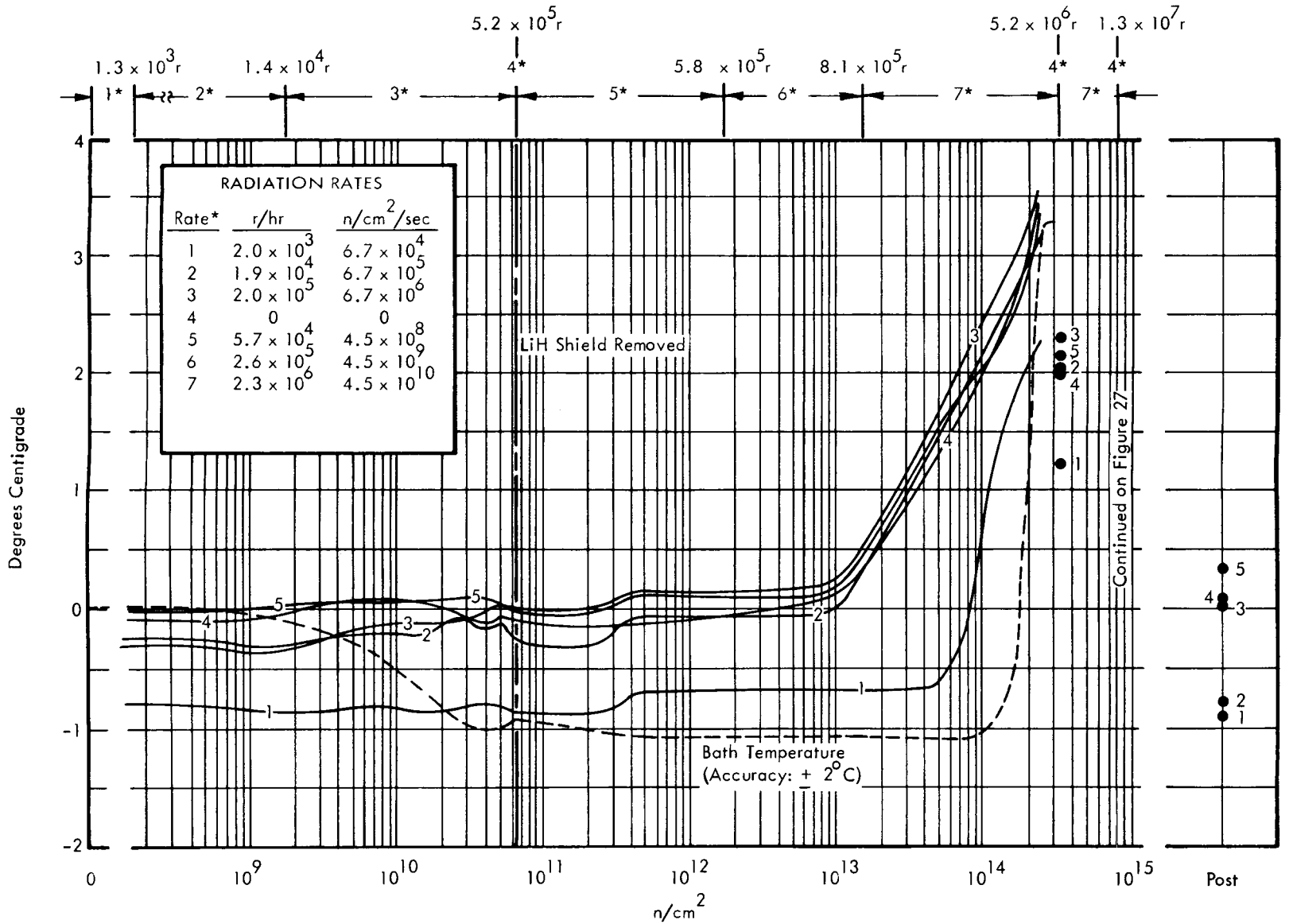

FIGURE 26 THERMISTOR R172, GENERAL ELECTRIC, TEMPERATURES VERSUS INTEGRATED NEUTRON FLUX

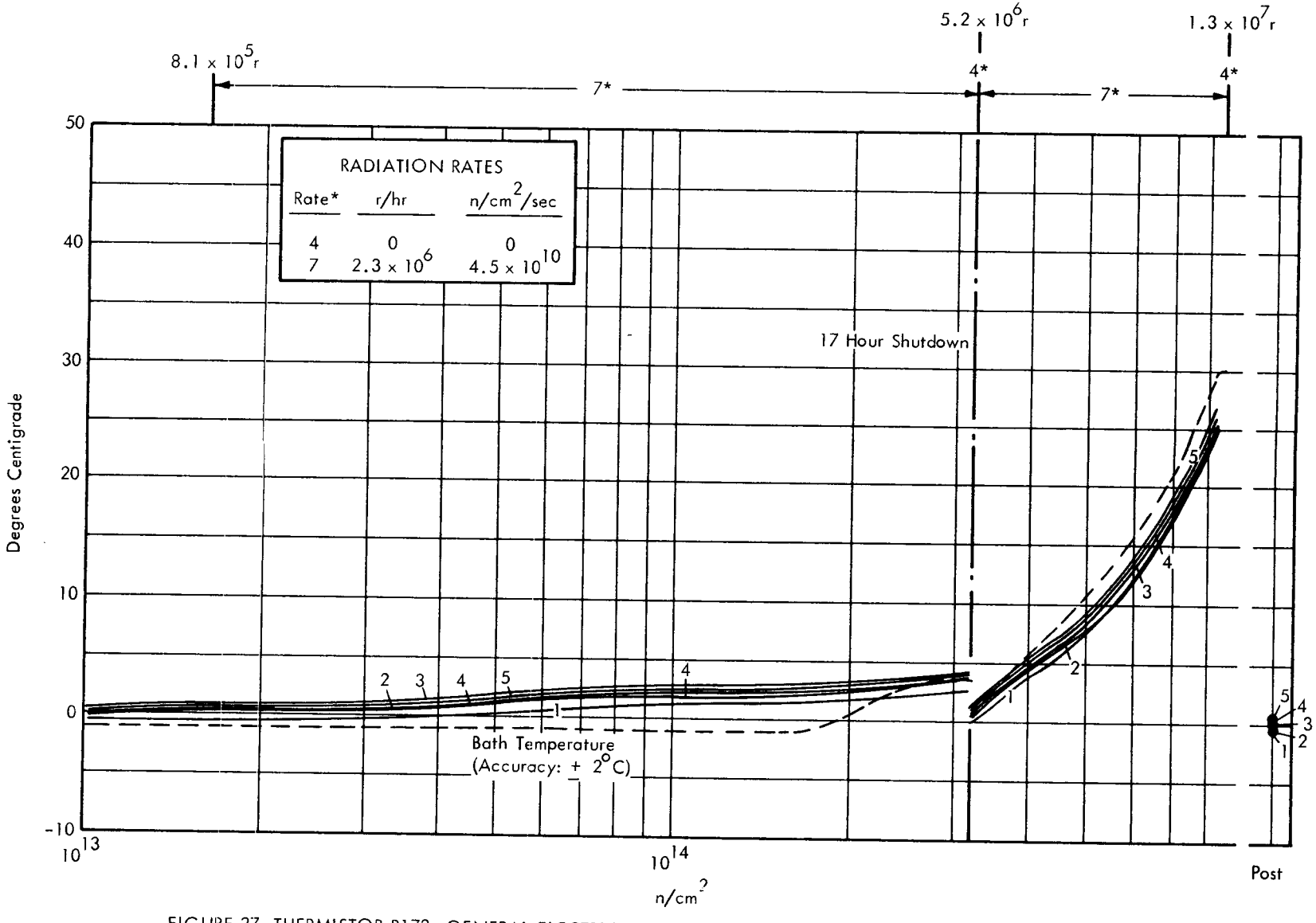

FIGURE 27 THERMISTOR R172, GENERAL ELECTRIC, TEMPERATURES VERSUS INTEGRATED NEUTRON FLUX

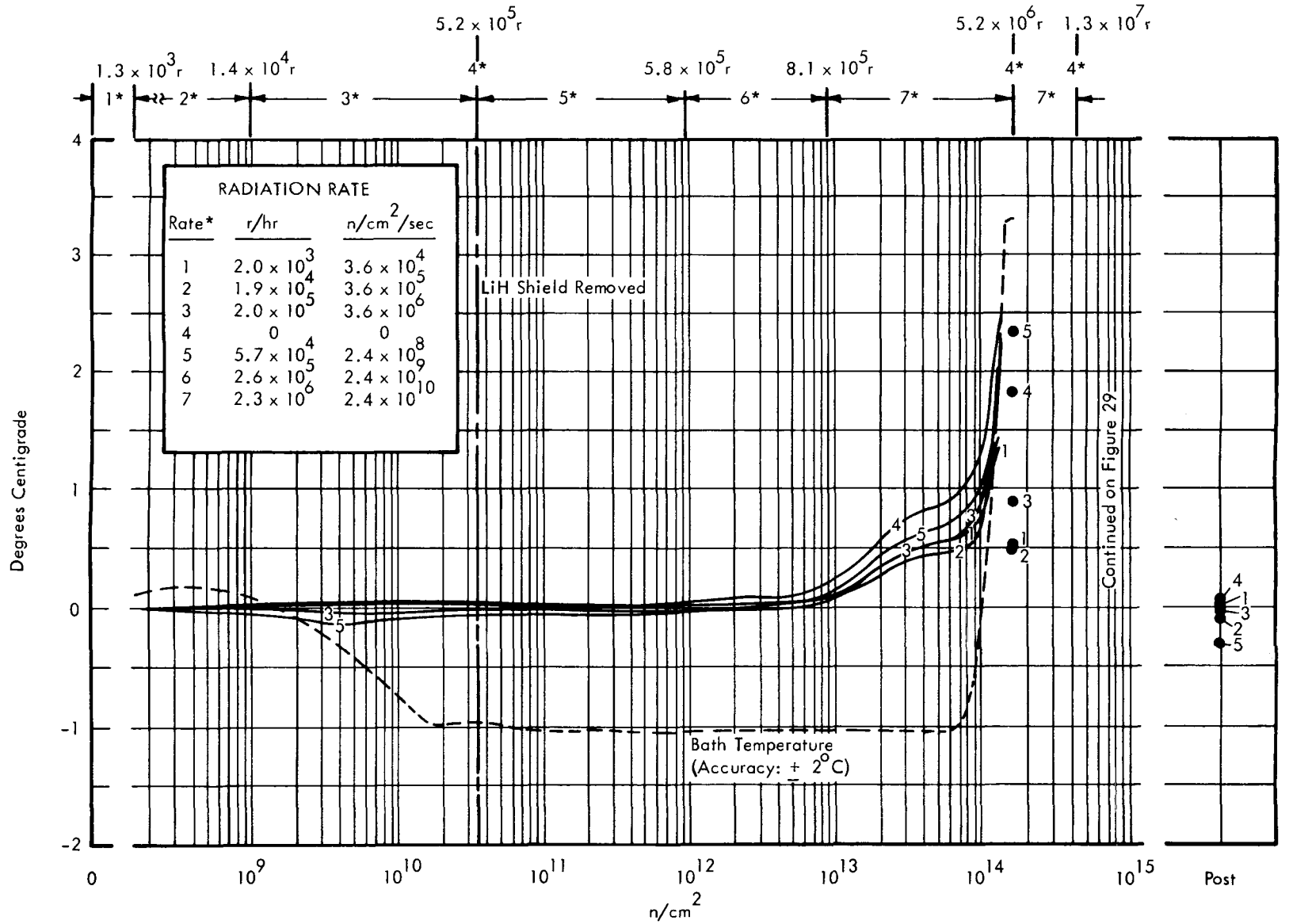

FIGURE 28 THERMISTOR GB31L1, FENWAL, TEMPERATURES VERSUS INTEGRATED NEUTRON FLUX

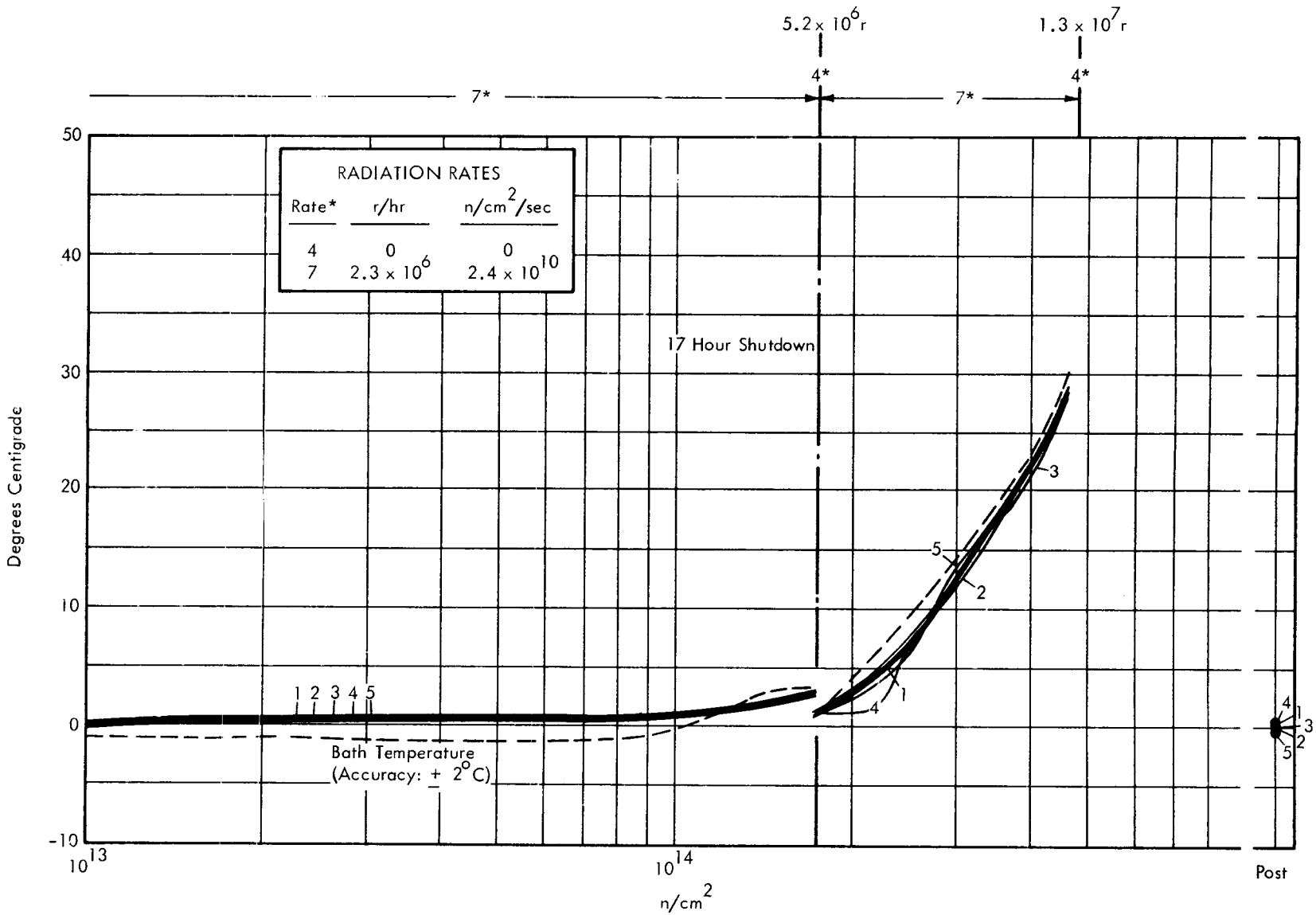

FIGURE 29 THERMISTOR GB31L1, FENWAL, TEMPERATURES VERSUS INTEGRATED NEUTRON FLUX

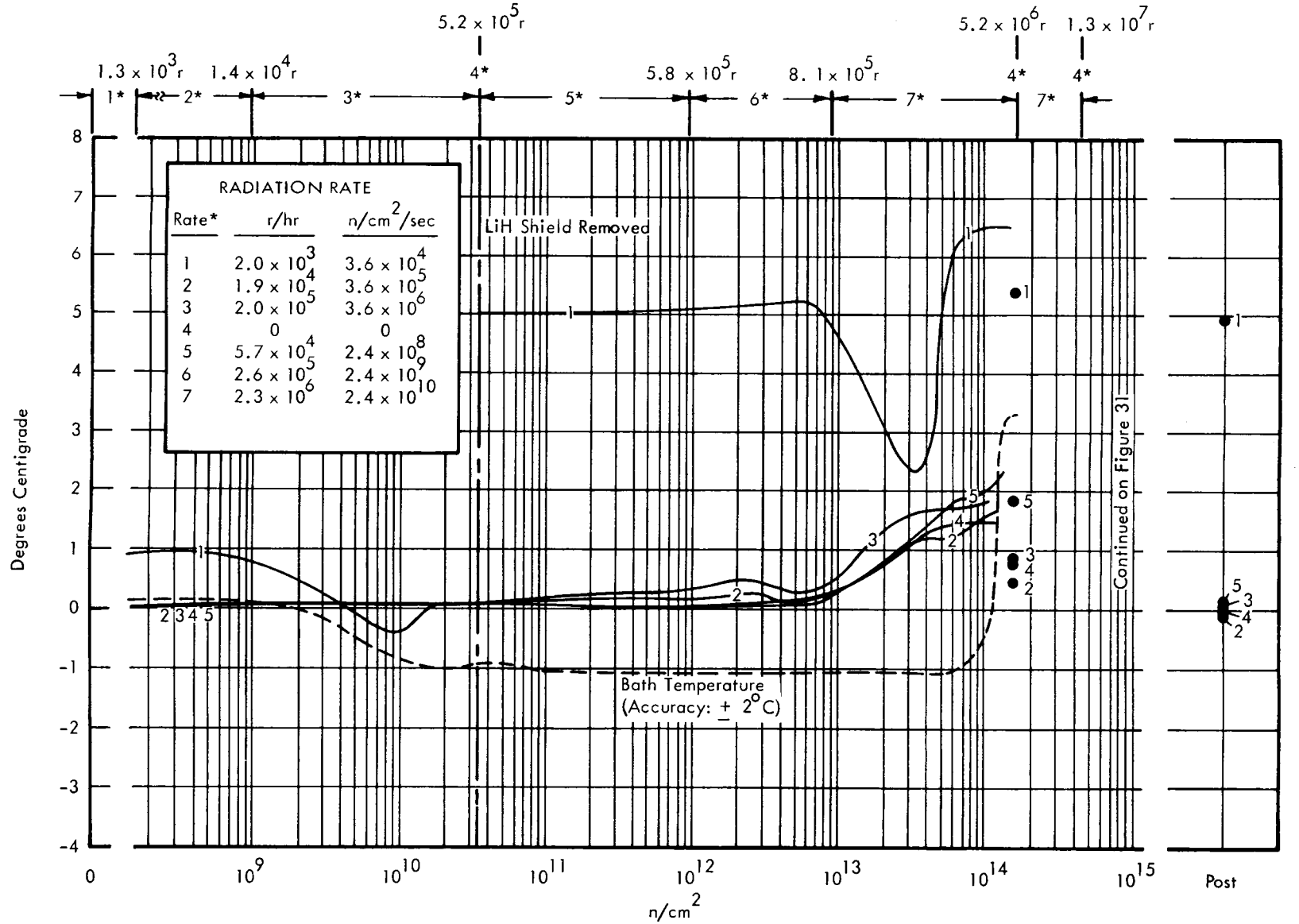

FIGURE 30 THERMISTOR GB41L1, FENWAL, TEMPERATURES VERSUS INTEGRATED NEUTRON FLUX

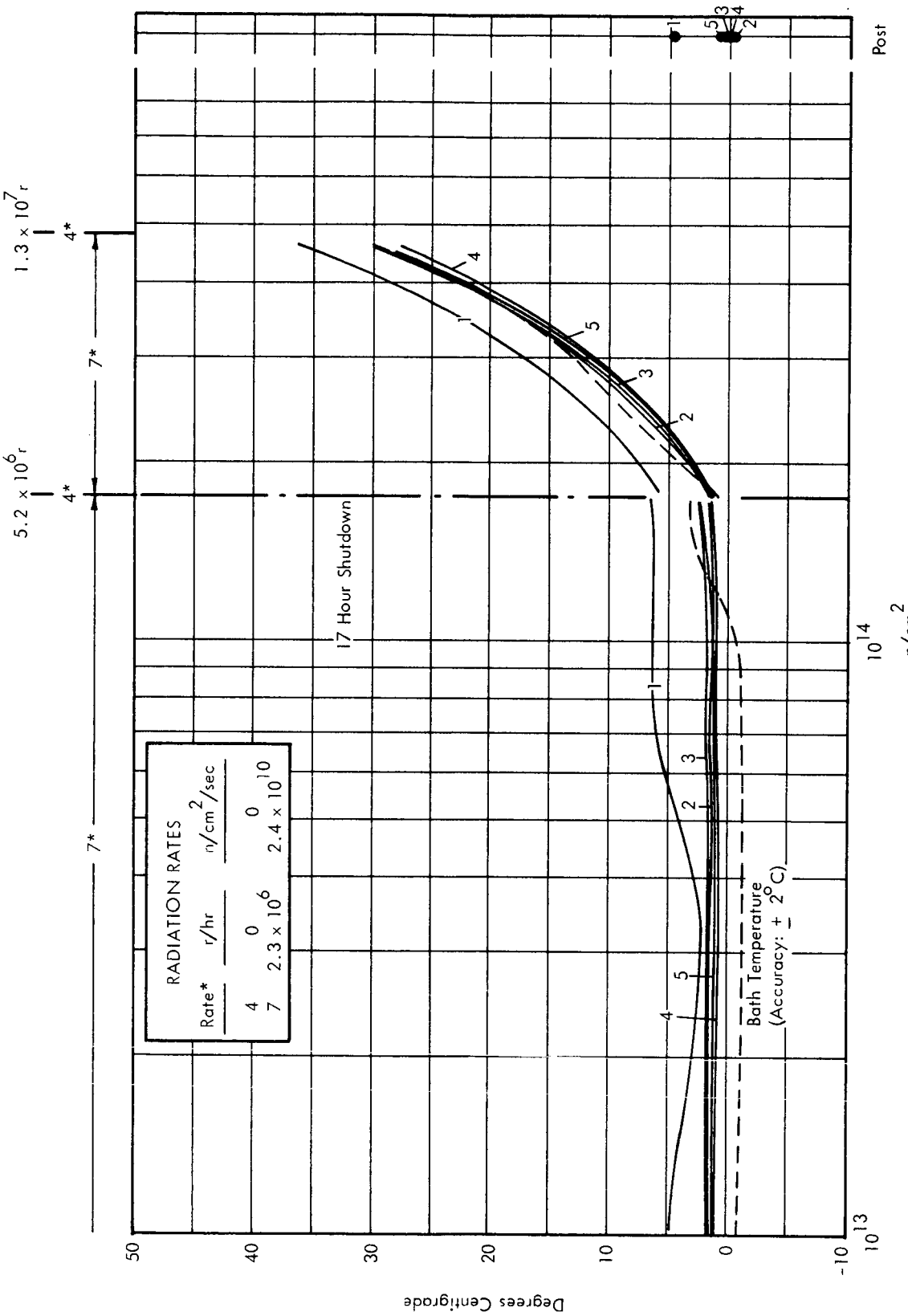

FIGURE 31 THERMISTOR GB41L1, FENWAL, TEMPERATURES VERSUS INTEGRATED NEUTRON FLUX

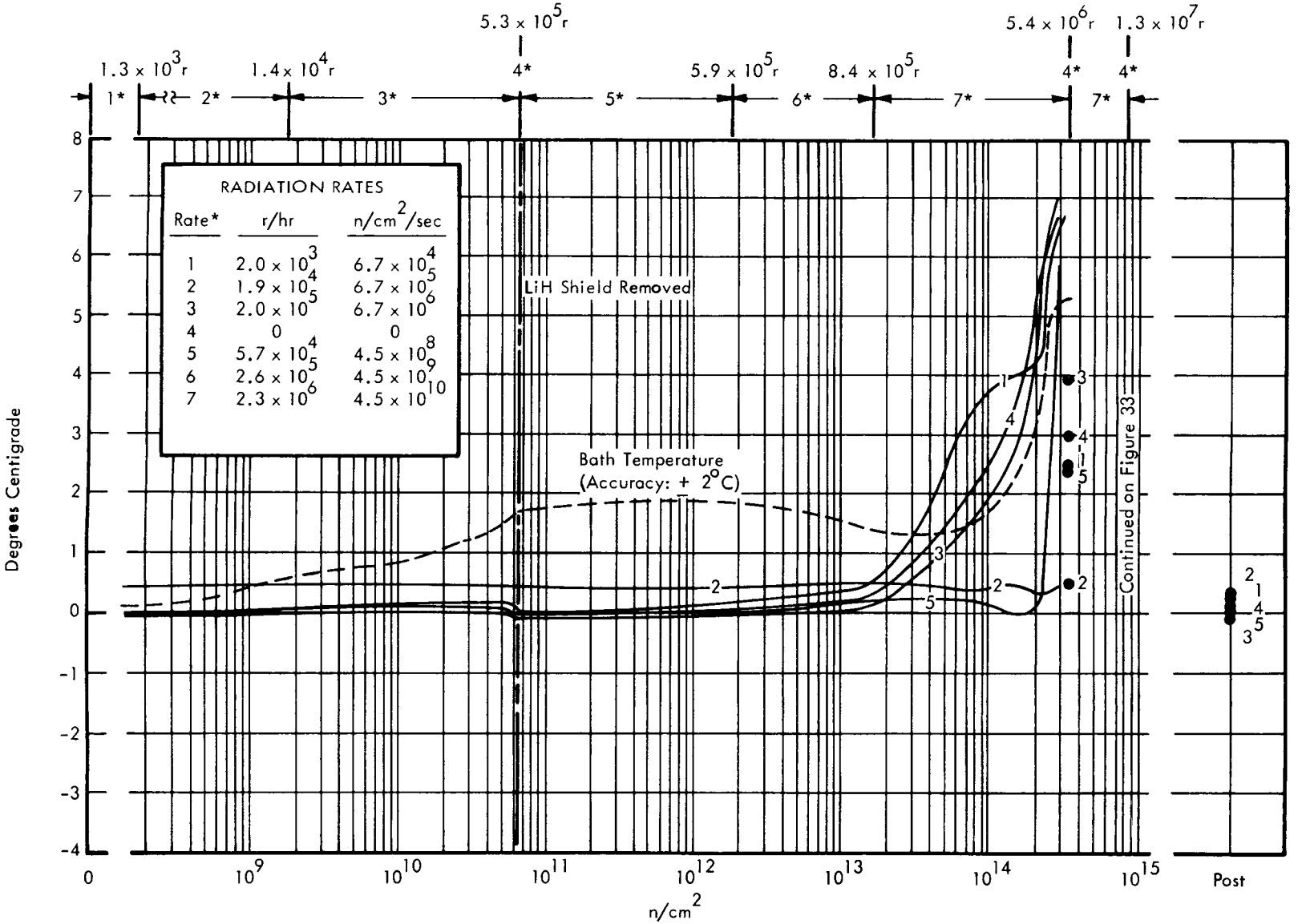

FIGURE 32 THERMISTOR RL13M1, KEYSTONE, TEMPERATURES VERSUS INTEGRATED NEUTRON FLUX

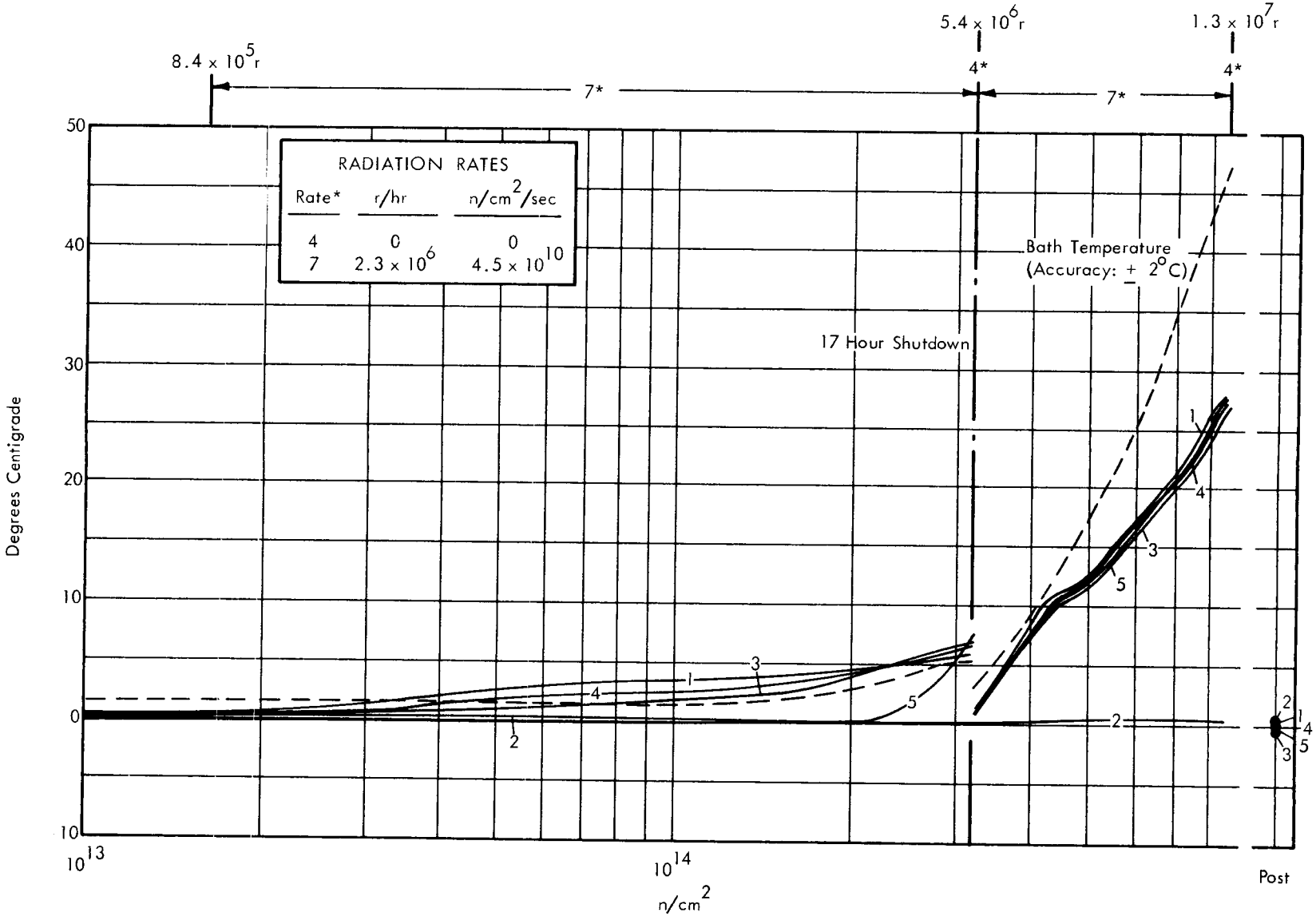

FIGURE 33 THERMISTOR RL13M1, KEYSTONE, TEMPERATURES VERSUS INTEGRATED NEUTRON FLUX

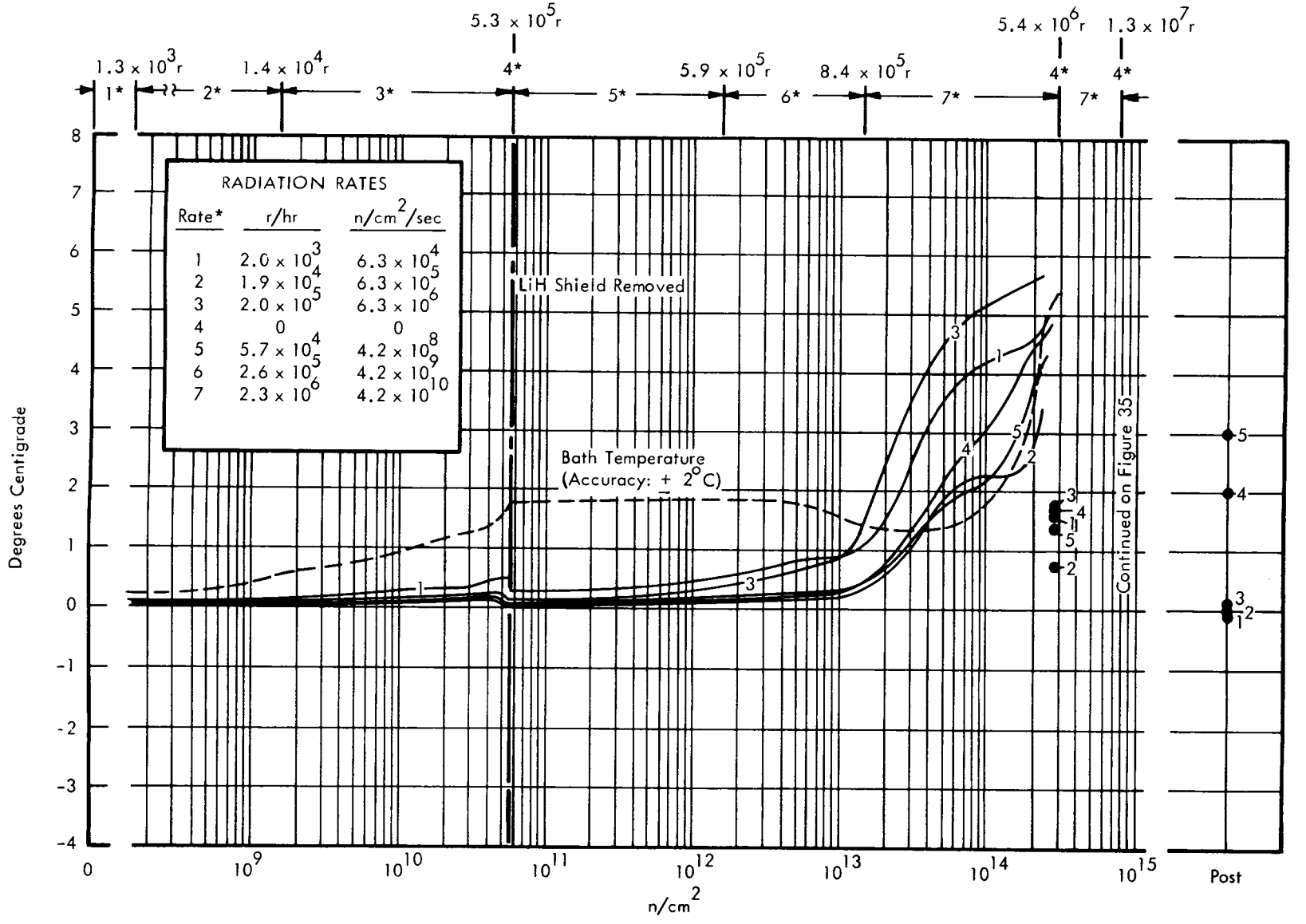

FIGURE 34 THERMISTOR RL20E1, KEYSTONE, TEMPERATURES VERSUS INTEGRATED NEUTRON FLUX

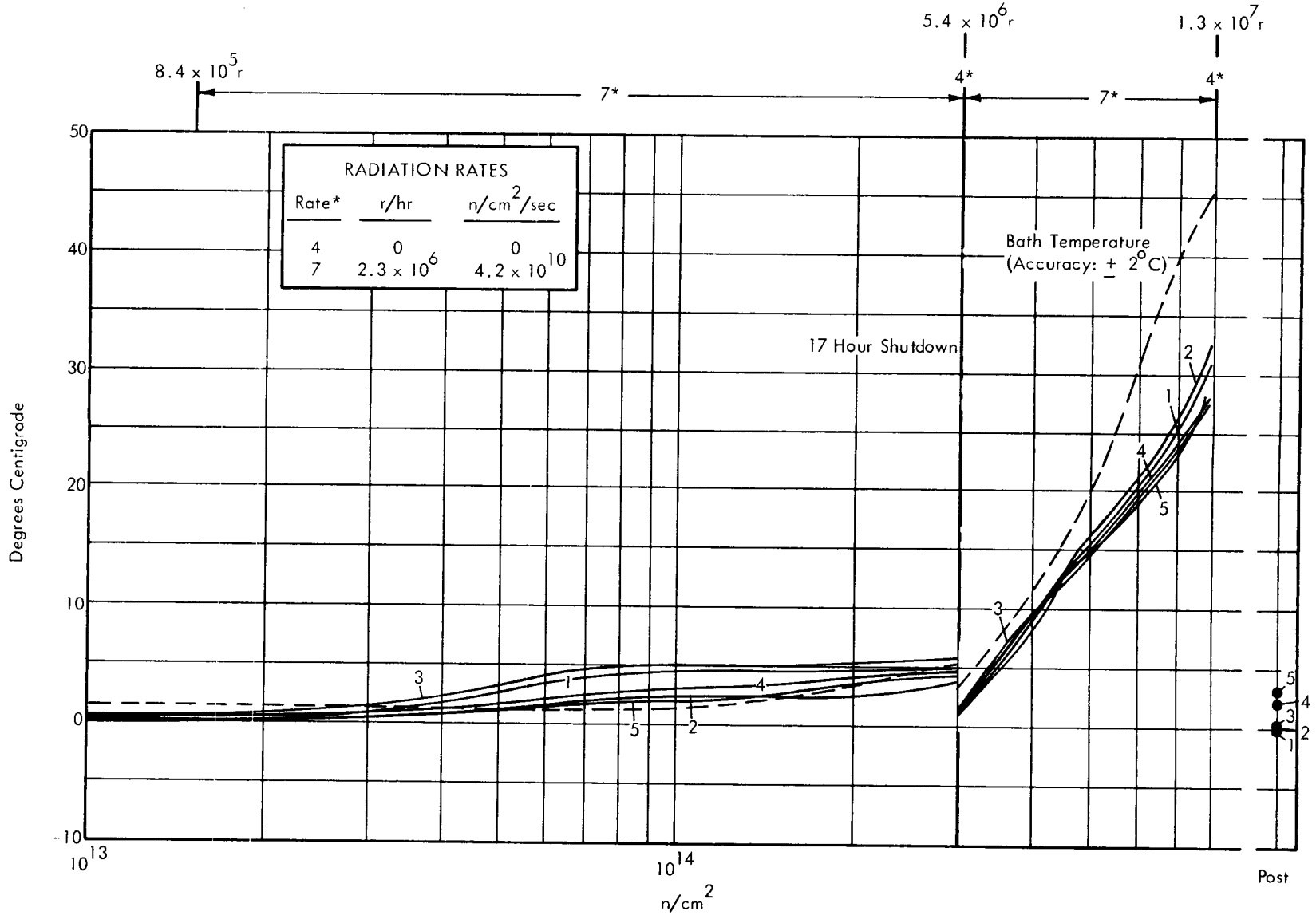

FIGURE 35 THERMISTOR RL20E1, KEYSTONE, TEMPERATURES VERSUS INTEGRATED NEUTRON FLUX

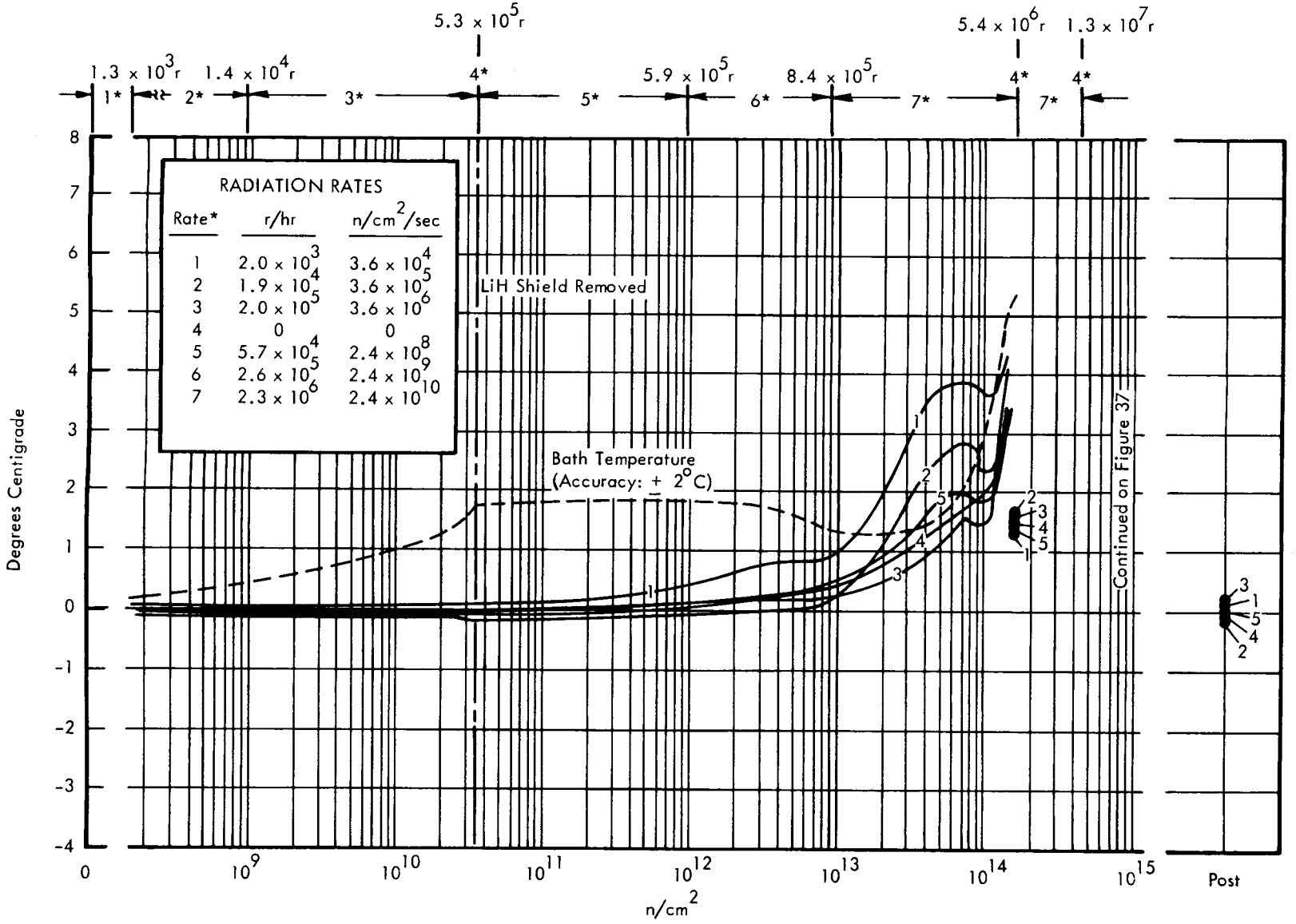

FIGURE 36 THERMISTOR RL4M1, KEYSTONE, TEMPERATURES VERSUS INTEGRATED NEUTRON FLUX

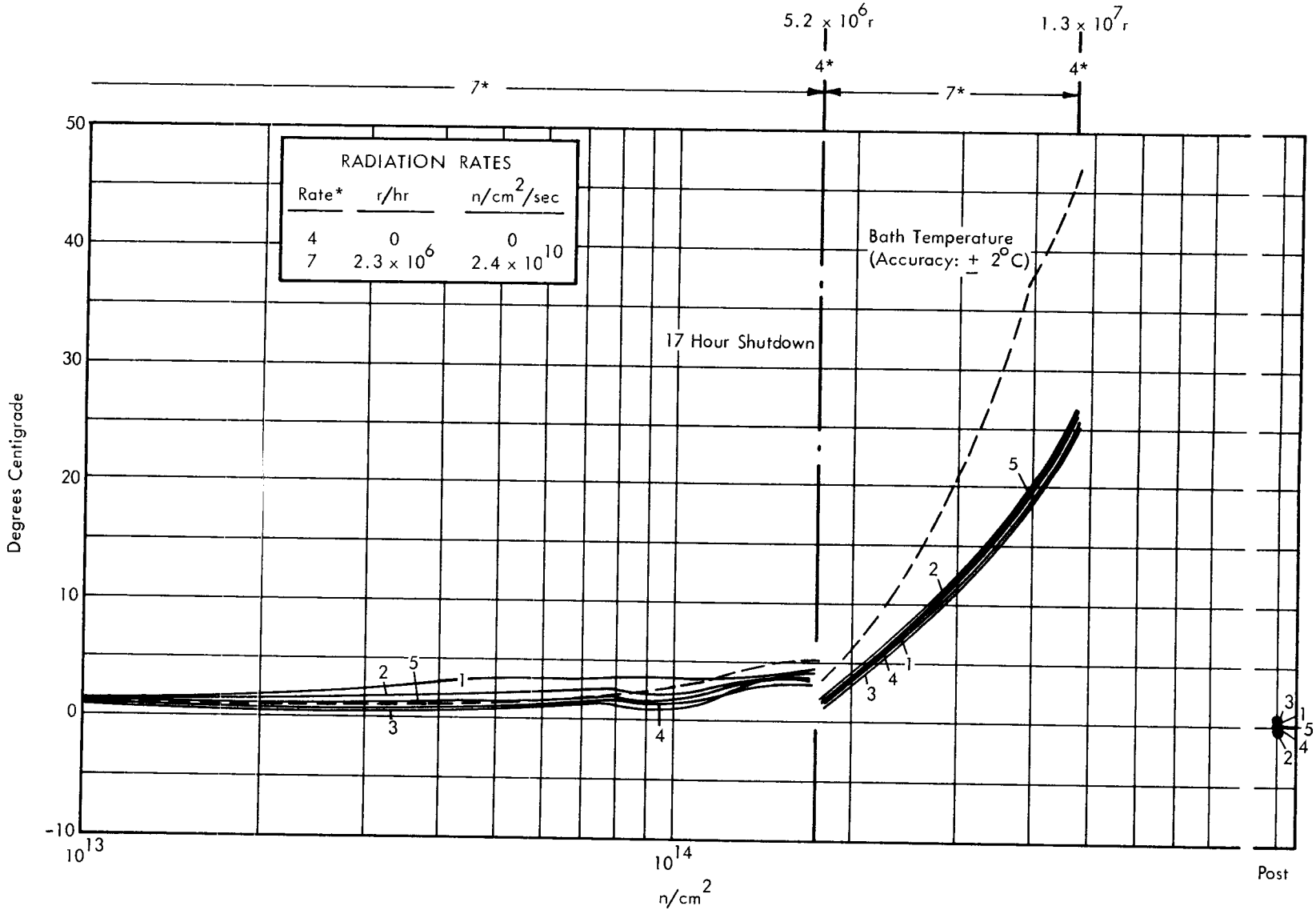

FIGURE 37 THERMISTOR RL4M1, KEYSTONE, TEMPERATURES VERSUS INTEGRATED NEUTRON FLUX

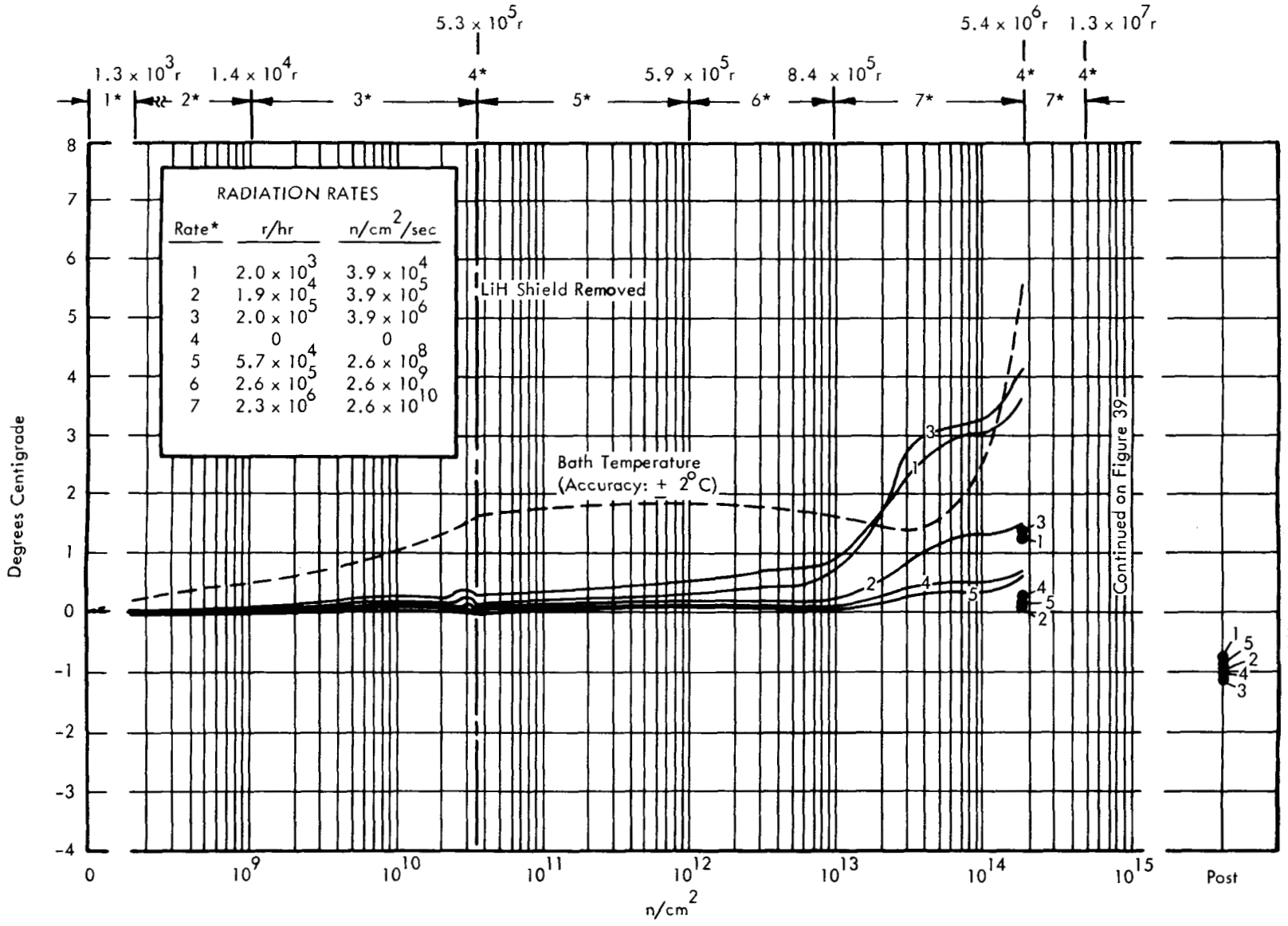

FIGURE 38 THERMISTOR RL7E1, KEYSTONE, TEMPERATURES VERSUS INTEGRATED NEUTRON FLUX

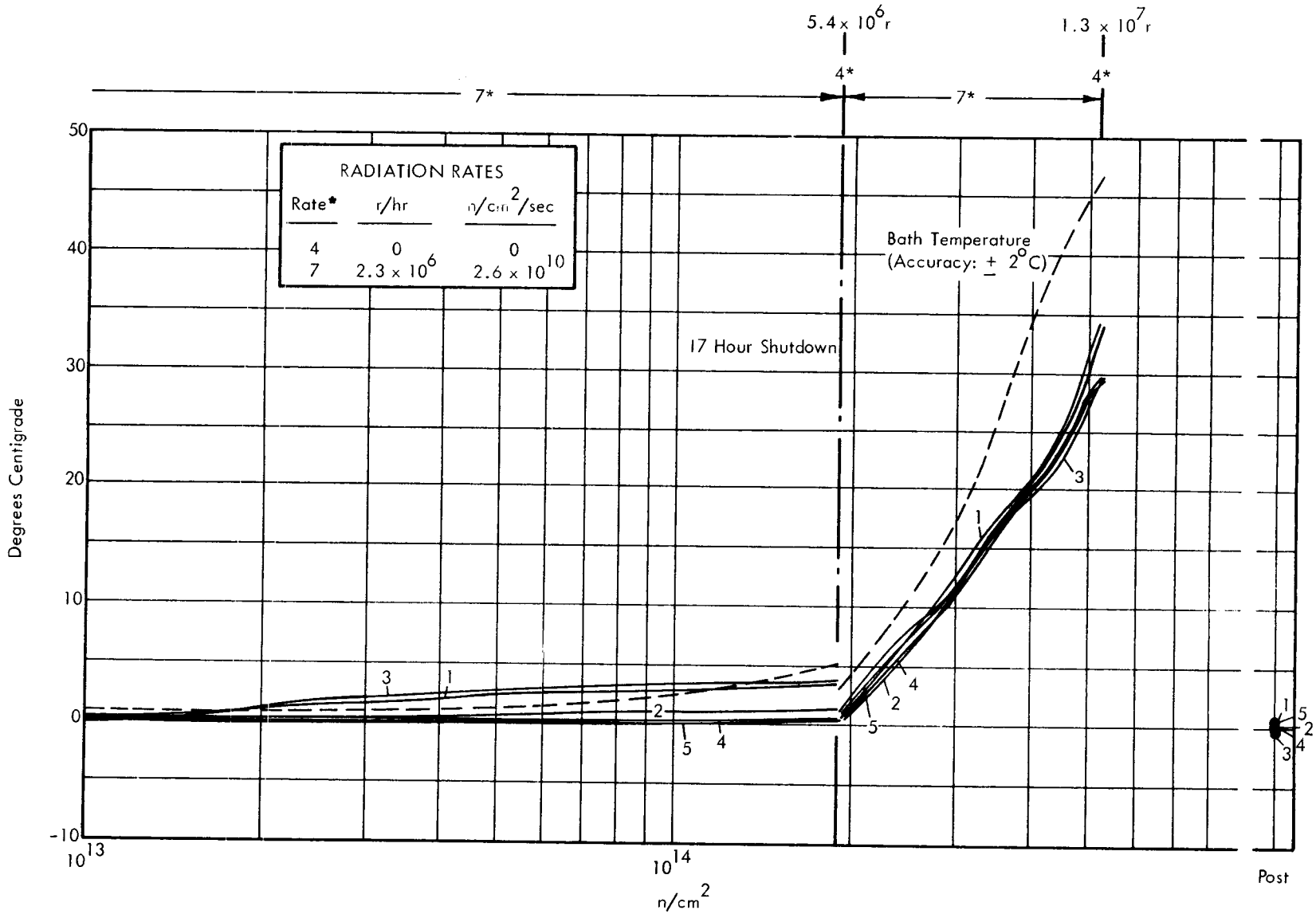

FIGURE 39 THERMISTOR RL7E1, KEYSTONE, TEMPERATURES VERSUS INTEGRATED NEUTRON FLUX